UNIVERSITÉ DU QUÉBEC À MONTRÉAL

NORTH AMERICAN GROUND SURFACE TEMPERATURE HISTORIES : A CONTRIBUTION TO THE PAGES2K NORTH AMERICAN PROJECT

THESIS

PRESENTED

AS PARTIAL REQUIREMENT

OF THE MASTERS OF ATMOSPHERIC SCIENCES

BY

FERNANDO JAUME SANTERO

NOVEMBER 2016

UNIVERSITÉ DU QUÉBEC À MONTRÉAL

HISTOIRE DE LA TEMPÉRATURE À LA SURFACE DU SOL DE L'AMÉRIQUE DU NORD: UNE CONTRIBUTION AU PROJET PAGES NAM2K

MÉMOIRE

PRÉSENTÉ

COMME EXIGENCE PARTIELLE

DE LA MAÎTRISE EN SCIENCES DE L'ATMOSPHÈRE

PAR

FERNANDO JAUME SANTERO

NOVEMBRE 2016

ACKNOWLEDGEMENTS

In first place, I have to thank my thesis directors, Dr. Hugo Beltrami, Dr. Jean-Claude Mareschal and Dr. Laxmi Sushama for giving me the opportunity to make this work possible.

Furthermore, I would like to thank my office colleages and friends Ignacio and Lidia for the great times we passed together. Thank you to Hugo Beltrami and Jean-Claude Mareschal for guiding me through the learning process of interesing topics such as paleoclimate and climate change as well as the technical advices in order to reconstruct and assess the climate histories obtained from subsurface thermal profiles.

My recognitions to the UQÀM sciences faculty for its financial support as well as the NSERC CREATE training program in climate sciences. This CREATE (TPCS) training program is administered at Saint Francis Xavier University with the cooperation of UQÀM among other universities. This CREATE TPCS is funded by the Natural Sciences and Engineering Research Council of Canada.

Moreover, I also want to thank the Geotop Research Centre in Geochemistry and Geodynamics for all the activities and students congresses that I was able to participate.

Finally, I would like to give thanks to all my friends and family, specially my mother Marisa, my sister Clara and my "chief commander" Carolyne. Thank you for supporting and trusting me, without your effort this adventure would not had been possible.

Arrieros somos, y en el camino nos encontraremos.

FOREWORD

The research work presents, integrally the masters thesis which I submitted the summer of 2016 in the Department of Earth and Atmospheric Sciences at Université du Québec à Montréal as partial requirement of the master of sciences in atmospheric sciences.

This research thesis is composed by a general introduction of the topic, followed by two articles and a general conclusion. The thesis is written in english with a french *résumé* attached. With the goal of submitting articles to scientific journals, they are presented to satisfy the criteria for international rules of publication, with summaries at the beginning and the tables and figures at the end.

The first article's title is *North American database for borehole temperature reconstructions* and the second article's title is *North American regional climate reconstruction from Ground Surface Temperature Histories.* The writing of these articles resulted from the collaboration between my thesis co-directors, Dr. Jean-Claude Mareschal professor of geophysics in the Atmorpheric and Earth sciences department at UQÀM and part of GEOTOP research center, and Hugo Beltrami who holds a Canada research Chair in Climate Dynamics at St. Francis Xavier University, he is an associate professor in the Department of Earth and Atmospheric Sciences at UQÀM.

TABLE OF CONTENTS

LIST OF TABLES

LIST OF FIGURES

LIST OF ABBREVIATIONS AND ACRONYMS

BH	Borehole
BTP	Borehole Temperature Profile
CE	Common Era
GST	Ground Surface Temperature
GSTH	Ground Surface Temperature History
LIA	Little Ice Age (1500-1800)
NAm	North America
NH	Northern Hemisphere
PAGES	Past Global Changes
SAT	Surface Air Temperature
SQL	Structured Query Language
SVD	Singular Value Decomposition
YBP	Years Before Present

RÉSUMÉ

Dans le cadre du projet PAGES NAm2k, 514 profils de température, mesurés dans des forages, ont été analysés pour le climat récent en l'Amérique du Nord. Les profils thermiques sélectionnés ont été enregistrés dans une base de données SQL. Pour faciliter les comparaisons et afin d'examiner la même période de temps, les profils ont été tronqués à 300 m. Les histoires de la température à la surface du sol pour les 500 dernières annés ont été obtenues par inversion de l'anomalie de température en utilisant la méthode de décomposition en valeurs singulières afin d'obtenir les changements de température durant 10 intervalles de temps de durée variable. Les inversions ont été filtrées pour quatre valeurs singulières et les histoires ont été décalées dans le temps en fonction de l'année où les forages ont été mesurés. La température de surface de référence et le gradient thermique ont été calculés par régression linéaire pour les derniers 100 mètres avec un intervalle de confiance de 95%. De plus, une méthode de Monte Carlo a été appliquée afin de trouver un ensemble de solutions à l'intérieur d'une marge d'erreur donnée par la différence quadratique moyenne entre le modèle et les données. Les reconstructions ont ensuite été modélisées directement afin d'assurer qu'elles sont à l'intérieur de la marge d'erreur maximale. Une analyse régionale a été réalisée pour reconstruire les variations de température moyenne tous les 50 ans au cours des 5 derniers siècles. Les résultats des modèles acceptés, donnés par la température moyenne et l'erreur de 2σ présentent, dans la plupart des cas, un réchauffement de $1°C$ à $2.5°C$ au cours des 100-150 dernières années.

MOTS-CLÉS: changement climatique, paléoclimatologie, histoires de la température à la surface du sol, réchauffement, PAGES2k

ABSTRACT

Within the framework of the PAGES NAm2k project, 514 North American temperature depth profiles were analyzed to infer recent climate changes. The selected profiles were saved inside a SQL database. The ground surface temperature (GST) histories for the last 500 years were reconstructed from the subsurface temperature anomalies using a singular value decomposition (SVD) inversion that retains four principal components and takes into account time logging differences. Steady-state surface temperature and thermal gradient were estimated by linear regression for the lower 100 meters of the temperature profile, and climate induced subsurface temperature anomalies were estimated as departures from the steady-state conditions. In addition, a Monte-Carlo method was applied to find the range of acceptable solutions within a maximum error interval between the forward modelled reconstruction and the profile. A regional analysis was performed for the last 5 centuries yielding mean temperature change every 50 years. The results, presented as the mean and 2σ distance of 500 accepted models, show a warming by 1.0°C to 2.5°C during the post industrial era.

KEYWORDS: climate change, ground surface temperature histories, PAGES2k, paleoclimatology, warming.

INTRODUCTION

The climate of our planet is determined by the balance of incoming and outgoing radiation in the upper atmosphere. Weather and climate emerge from any energy imbalance which results from the difference between the energy absorbed by the atmosphere and the energy emmited to outer space (Hansen *et al.*, 2005, 2011; von Schuckmann *et al.*, 2016). Climate forcings are defined as natural or human induced perturbations of the energy balance originated outside the climate system. The oceans and the atmosphere, among other climate subsystems, are sentistive to those changes in the energy budget which are translated in a sequence of climate changes such as global warming (Allan *et al.*, 2014; Trenberth *et al.*, 2014). With the present increase of the global mean temperature, an understanding of the past climate and its variability during the last millennium has become imperative in order to gain insights into present and future climate changes.

The key to understanding the impacts of human activity over the climate system resides in the ability to distinguish between its natural variability and the possible changes induced by human activity. General circulation models (GCMs) have become useful tools to forecast future climate trends under various scenarios defined by different climate forcings. However, GCMs must be compared with robust past climate reconstructions to asses their simulations and improve their outputs(González-Rouco *et al.*, 2009; PAGES 2k-PMIP3 group, 2015; Smith *et al.*, 2015).

As meteorological records only cover a small fraction of the Earth's climatic history, they are too short to give a longer perspective on climate variability. Nev-

ertheles, climate-dependent natural phenomena provide an indirect approach to reconstruct and understand past global changes. Therefore, climate histories obtained from paleoclimate recorders are used to study past climate changes. It is the study of these proxy indicators that forms the foundation of paleoclimatology (2k Consortium, 2013).

Data records extracted from ice cores (Oeschger and Langway, 1989; Bauer *et al.*, 2013; Thompson *et al.*, 2013), tree rings (Douglass, 1919; Briffa *et al.*, 1990; George and Ault, 2014), pollen (Davis *et al.*, 2003; Viau *et al.*, 2012; Jacques *et al.*, 2015) and boreholes (Mareschal and Beltrami, 1992; Bodri and Cermak, 2007; Beltrami *et al.*, 2014), among others, are commonly used for past climate reconstructions. All of them have different resolutions and may be sentitive to different factors. For instance, tree ring reconstructions have better short temporal resolution(annual) than borehole temperature inversions (multidecadal), but due to standardization, long tree-ring chronologies may not reconstruct long-term climate variability properly (Briffa and Osborn, 1999).

On the other hand, borehole climatology assumes that surface air temperature (SAT) and ground surface temperature GST are coupled, and their changes induce perturbations that propagate through the subsurface by heat conduction (Harris and Chapman, 1998a,b; García-García *et al.*, 2016), neglecting the advection term.

Temperature-depth profiles measured in boreholes have commonly been used by geophysicists to study the Earth's heat flux (Bullard, 1939; Benfield, 1939). In the 1930's, Hotchkiss and Ingersoll attempted to infer past climate from temperature-depth profiles (Hotchkiss and Ingersoll, 1934). It was only in the 1970s that systematic studies to infer past climate from borehole temperature profiles (BTPs) were undertaken (Cermak, 1971; Sass *et al.*, 1971; Beck, 1977). With the concern about warmer global temperatures, studies have become more widespread,

including local and global analyses (Beltrami *et al.*, 1992; Clauser and Mareschal, 1995; Mareschal *et al.*, 1999; Huang *et al.*, 2000; Pickler *et al.*, 2016b). Several regional analyses have been undertaken in North America (Gosnold *et al.*, 1997; Majorowicz *et al.*, 2002; Chouinard *et al.*, 2007) but none of them has analyzed the entire continent in detail. Following that line, the study presented in this thesis aims at filling this gap by performing a regional analysis of past GST changes in North America for the past 5 centuries.

The first part of the study was the collection of a database with thermal profiles suitable for climate reconstructions. A data collection of thousands of thermal profiles was accomplished in order to assess their quality. The main reason for this data selection is that most of those profiles were measured for heat flux studies, and might not be adequate for climate purposes. Reasons for rejection were for instance, the detection of ground water flow and conductivity changes that might alter the climate signal recorded as a perturbation from the geothermal steady-state, an insufficient depth range, less that 100 meters and deeper than 300 meters for a reconstruction of the past 5 centuries). Selected borehole temperature profiles were put in a public database and the whole process is described in the first article (Chapter 1), *North American database for borehole temperature reconstructions.*

Furthermore, within the framework of PAGES2k project, more than 500 borehole temperature-depth profiles selected from North America were analyzed to reconstruct the GST histories for the past 5 centuries. Steady-state surface temperature and thermal gradient were estimated by linear regression for the lower 100 meters of the temperature profile, and climate induced subsurface temperature anomalies were estimated as departures from the steady-state conditions. The GST histories for the past 500 years were reconstructed from the subsurface temperature anomalies using a singular value decomposition (SVD) inversion. Additionally, a Monte-Carlo inversion was performed to find the range of solutions within a max-

imum subsurface anomaly error determined by the root mean square difference between the model and the data. A regional analysis was performed for the last 5 centuries yielding mean temperature change every 50 years. The GST history results, presented as the mean and 95% confidence interval, show a warming by 1.0°C to 2.5°C during the post industrial era. These reconstructions span the North American continent and allow for the examination of regional trends. This composes the second article *North American regional climate reconstruction from Ground Surface Temperature Histories* which is a contribution for PAGES2k, and will be published in Climate of the Past, *Special Issue: Climate of the past 2000 years: global and regional syntheses.* It is the base of this thesis (Chapter 2).

Finally, a GST reconstruction for the past 1000 years, obtained from boreholes truncanted at 500 meters, will be presented as an appendix where it is compared with the 500-year GST reconstruction studied in Chapter 2 as well as the surface temperature simulation of GISS-E2-R.

CHAPTER I

NORTH AMERICAN DATABASE FOR BOREHOLE TEMPERATURE RECONSTRUCTIONS

Fernando Jaume-Santero[1], Hugo Beltrami[2,3], Jean-Claude Mareschal[1]

[1]Centre de Recherche en Géochimie et en Géodynamique (GEOTOP), Université du Québec à Montréal, Montréal, Québec, Canada

[2]Climate & Atmospheric Sciences Institute and Department of Earth Sciences, St. Francis Xavier University, Antigonish, Nova Scotia, Canada

[3]Centre pour l'étude et la simulation du climat à l'échelle régionale (ESCER), Université du Québec à Montréal, Montréal, Québec, Canada

1.1 Abstract

Analyses of geothermal data from borehole temperature profiles are able to yield reconstructions of low-frequency temporal variations of the ground surface temperature. These ground surface temperature reconstructions form part of the paleoclimatic network that is suitable for validation of climate model simulations. Thus, we have increased the number of North American temperature depth profiles useful for temperature reconstructions from 245 in Huang, Pollack and Shen (2000) to 510 in the present database. These data are in a public database containing North American borehole temperature profiles deeper than 300 meters, that are suitable to reconstruct recent (500 years) low-frequency climate trends.

1.2 Background & Summary

General circulation model (GCM) simulations are very useful to forecast future climate projections under different predefined scenarios. However, because of the limited resolution of GCMs, many significant climate-involved processes driving at less than the GCM grid size scale are parameterized differently among model teams, therefore their outputs still have a large degree of uncertainty and they need to be compared with real climate data to assess their robustness and validate their outputs. As instrumental meteorological data are only available for the past 150 years, climate reconstructions for longer timescales require paleoclimatic data.

There is a wide diversity of paleoclimatic data within Earth's system such as tree rings, ice cores, pollen, lake sediments, or borehole temperature profiles , that have their own degree of spatial and temporal uncertainties. Paleoclimatic archives, such as those kept by the National Climate Data Center at NOAA, contain data from these indirect climate recorders that allow for the reconstruction of past climate trends for hundreds to thousands of years.

In borehole climatology (Bodri and Cermak, 2007; González-Rouco *et al.*, 2009), it is assumed that surface air temperature (SAT) and ground surface temperature (GST) are coupled(e.g. Harris and Chapman, 1998b, 2001). The changes in ground surface temperature propagate downward and are recorded as transient perturbations to the steady-state geothermal regime in the subsurface. Therefore, it is possible to estimate changes in ground surface temperature and infer past climate variations from the perturbations of the borehole temperature profiles (BTPs) (e.g. Beltrami *et al.*, 1992; Beltrami and Mareschal, 1993; Clauser and Mareschal, 1995; Huang *et al.*, 2000).

We present in a public database all the BTPs suitable for climate studies that can be used to perform a regional analysis of ground surface temperature histories for the past 500 years in North America. Our analysis will be included in the special volume of the PAGES NAm2k project along with other proxies to reconstruct the climate trends in North America for the Common Era.

1.3 Methods

Assuming a homogeneous subsurface in absence of non-climatic perturbations, temperature increases linearly with depth. Thus, heat flux can be considered as "steady-state" with respect to the time scales of climatic surface variations. Thermal profiles measured in boreholes have commonly been used by geophysicists to determine Earth's heat flux and estimate the geothermal "steady-state" (e.g. Bullard, 1939; Benfield, 1939). However, perturbations of underground temperatures by climate variations at the surface are clearly reflected in the thermal profile. These climate perturbations recorded in the subsurface must be extracted from the profile to infer past surface temperature trends. The quality of the profile for climate purposes will be determined by natural conditions at the location of the borehole such as the thermophysical properties of the subsurface, the topog-

raphy, or the hydrology, as well as requirements on the thermal profiles such as the minimum depth. Thousands of North American BTPs were passed through a selection process to assess whether they were suitable for climate reconstructions.

1.3.1 Data description

Temperature profiles measured in boreholes were obtained from the public databases listed in the Data Citations section. Borehole datasets consists of a set of subsurface temperatures $T(z)$ and associated depths (Figure 1.1). The measurement process consists of introducing a thermistor probe inside the borehole and taking measurements of the resistance at different depths (usually beneath the water table. Resistance ($k\Omega$) is usually measured every 10 meters (sometimes 50 feet). With the thermistor calibrated in the lab for the range of expected temperatures, temperatures are determined with an estimated accuracy on the order of 20 mK and a precision greater than 5 mK.

In addition to the BTP data, there are also metadata describing the features of the borehole such as the location, the diameter of the hole, thermal conductivity, heat production among many others. Information useful for climate reconstructions was included in the metadata table. See the Data Records section for more details. Information concerning the original contributors, is listed in the database under contacts for each BTP. When a contact name could not be found, the contact is listed as *unknown*.

1.3.2 Data selection

Many BTPs, published for heat flow studies, are available in public datasets. A list of such datasets for North American thermal profiles is provided in Table 1.1. However, not all of these profiles are suitable for climate reconstructions. Thus, each profile must satisfy a number of conditions before it is deemed suitable for

climate studies. There are many potential sources of non-climatic perturbations of the BTP that can affect the extraction of the geothermal steady-state and the reconstruction of past temperature changes at the surface. Therefore, several conditions are defined to ensure that the dataset contains clean thermal profiles without non climatic disturbances. The conditions that we have set are the following:

1. *Depth range:* Useful profiles must be deeper than 300 meters in order to be able to reconstruct for at least the past 500 years. The first measurement must have a minimum depth of 95 meters to be able to properly define the temperature perturbation of the past 100 years which usually dominates the climate signal.

2. *Number of measurements:* Each profile must contain at least 10 measurements.

3. *General check:* Temperature-depth profiles are plotted as in Figure 1.1 to eliminate profiles that exhibit obvious non-climatic disturbances such as water flow, or abrupt conductivity changes.

4. *Surface conditions near the borehole:* Many sources of non climatic perturbations can be observed at the surface (Chouinard and Mareschal, 2007). Recent deforestation can induce a local warming signal that is not due to climate change (Lewis and Wang, 1998). Other surface conditions affecting the temperature profile include topography (higher elevation producing an apparent warming signal), the presence of lake (profiles from holes inclined toward a lake giving an apparent cooling signal in Canada). Unfortunately, surface conditions have not been documented for the majority of the heat flow studies before 1980, and the selection was possible only for the most recent temperature profiles. .

Consequently, after selecting profiles from several datasets (Table 1.1), we only retained a small fraction of them (in total 510), and included them in this database. Their locations are shown on a map (Figure 1.2).

The distribution of the retained profiles is not uniform across North America. The Canadian Shield is very well sampled (at least its southern part) because it was the target of heat flow studies of the continental lithosphere, and because mining exploration holes are available to measure temperature depth profiles in crystalline rocks. Suitable profiles are absent from the Gulf coast region including Oklahoma and Texas. Sedimentary basins are often affected by water flow and thermal convection in the permeable sediments. Furthermore, temperature measurements in oil wells are made out of equilibrium during drilling. Wells that are not put in production are cemented to avoid contamination of aquifers, and not accessible for measurements. Very few profiles are found in the southwestern United States where many heat flux measurements have been made. In the Basin and Range Province, where heat flow is very high, shallow holes are sufficient to define a high temperature gradient. Furthermore most measurements in the Southwestern US were made in holes drilled in basins strongly affected by thermal convection. There is also a lack of useful deep profiles in Mexico and the Caribbean.

1.4 Data Records

The database presents 510 BTPs suitable for climate reconstructions and a metadata table containing useful information about each of them. They are publicly available in Figshare, DOI: `10.6084/m9.figshare.2062140`, and they can be downloaded from
`https://figshare.com/s/0a1d213c3814024c4333`. They can be found in two formats, as Comma-separated value (CSV) and as tabular-based files, which

are efficiently loaded with different research environments such as MATLAB, Jupyter/Python or R.

The CSV dataset is organized to be loaded with a spreadsheet.

The metadata table (METADATA.CSV) contains the following columns,

- **Name**: Borehole IDs.
- **Longitude**: Coordinate X longitude (decimalized)
- **Latitude**: Coordinate Y latitude (decimalized)
- **Logging Year**: The year(s) when the borehole was measured.
- **Contact**: Person or group who logged the profile.
- **Country**: The country where the borehole was drilled.
- **Thermal conductivity**
- **Max. Depth**: Maximum logged depth.
- **Data number**: Number of measurements for each BTP.

The coordinates have been decimalized. The accuracy of the location depend on the age of the measurement. For the the oldest data the location is accurate to a minute; for the recent data, the location accuracy is better than a tenth of a second. Each temperature profile is contained in an individual CSV file identified with the borehole name.

The data are in two columns:

- **Depth_m**: The depth (z) in meters.
- **Temperature_Celsius**: The temperature ($T(z)$) in degrees Celsius.

The same data scheme is followed for the profiles in the TABULAR database. Their metadata appear as comments (preceded by #) in the same file as the temperature-depth measurements.

1.4.1 Computer Program

Short computer programs are included in the data package. They show examples of how to load the profiles and metadata contained in the database. The example codes are: *load_data.m* Matlab/Octave code that loads the temperature-depth profile from CSV files, *load_data.py* Python 3 script that loads the temperature-depth profile as well as the metadata for a given borehole in the TABULAR database and *meta_panda.ipynb*, Ipython code that loads the entire metadata file, using Pandas, the python data analysis library. Furthermore, CSV is a multi-platform format that can be directly loaded by spreadsheet-based programs such as EXCEL or Open Office.

1.5 Validation test

A test was performed to check the consistency of the profiles truncated at 300 meters. Reference surface temperatures (T_0) were obtained by the intercept of the linear regression to the lowermost 100 meters of the temperature profiles (T(200m) to T(300m)). A map of the reference temperatures and plot of temperature *vs* latitude is shown on Figure 1.3. The temperature decreases with increasing latitude, as expected.

1.6 Usage Notes

This borehole database is published to be used for a North American regional analysis from ground surface temperature histories using temperature-depths profiles suitable for climate reconstructions. Several methods for inversion of these data have been proposed by different research groups: Backus-Gilbert method (Vasseur *et al.*, 1983), functional space inversion (Shen and Beck, 1991), singular value decomposition (Mareschal and Beltrami, 1992), Monte-Carlo method (Mareschal *et al.*, 1999). A discussion and comparison between some of the methods can be found in Beck *et al.* (1992). The same methods can also be applied for simultaneous inversion of all the data from a given region. Computer programs implementing the inversion algorithms can be requested from the researchers. The database could also be useful to study spatial differences of conductivity in North America. Conductivities obtained from 453 boreholes vary from 0.87 W/mK to 7.23 W/mk as shown in Figure 1.4. This is a parameter that takes very different values in different climate models. As a first approach, no regional conductivity patterns are discerned. However, a more complete study of the spatial distribution of thermal conductivities could be done by adding those boreholes shallower than 300 meters.

1.7 Acknowledgements

Many researchers have been involved in the collection of the data included in this compilation. A probably incomplete list includes A. Judge, A. Taylor, A.H. A. Beck, Lachenbruch, A.M. Jessop, D.D. Blackwell, D. Chapman, E.R. Decker , F. Birch, F.E. Urban, G. Clow, H.N. Pollack, J. Heine, J. Majorowicz, C. Jaupart, J.C. Mareschal, G. Bienfait, C. Pinet, L. Guillou, F. Rolandone, C. Gosselin, F. Levy, C. Phaneuf, C. Pickler, C. Chouinard, J.H. Sass, K. Wang, L. Larry, M. Severson, P. Morgan, R. Roy, R. Scatollini, R.N. Harris, S.R. Durrans, T. Lewis, V. Cermak, W.D. Gosnold, W.H. Benkowski, W.H. Diment. We apologize to those who have been left out. This work was supported by grants from the Natural Sciences and Engineering Research Council of Canada Discovery grant (NSERC DG 140576948) and the Canada Research Program (CRC 230687) to H. Beltrami. Computational facilities were provided by the Atlantic Computational Excellence Network (ACEnet-Compute Canada) with support from the Canadian Foundation for Innovation. H. Beltrami holds a Canada Research Chair in Climate Dynamics. FJS is funded by a graduate fellowship from a NSERC-CREATE Training Program in Climate Sciences based at St. Francis Xavier University.

1.8 Competing financial interests

The authors declare no competing financial interests.

1.9 Data Citations

See Table B.1 and supplementary material.

Table 1.1 Data sources from where the temperature-depth profiles were taken.

Source name	Availability
University of Michigan	`http://www.earth.lsa.umich.edu/`
SMU Geothermal Lab	`http://geothermal.smu.edu/`
GEOTOP database	`http://www.geotop.ca/`
NOAA borehole datasets	Huang *et al.* (1999)
USGS array	`www.aoncadis.org/dataset/USGS_DOI_GTN-P/`
Canadian geothermal data compilation	Alan M. Jessop et al.
Jean-Claude Mareschal's data book	Jean-Claude Mareschal
Richard Scattolini, Ph.D. thesis Scattolini (1978)	

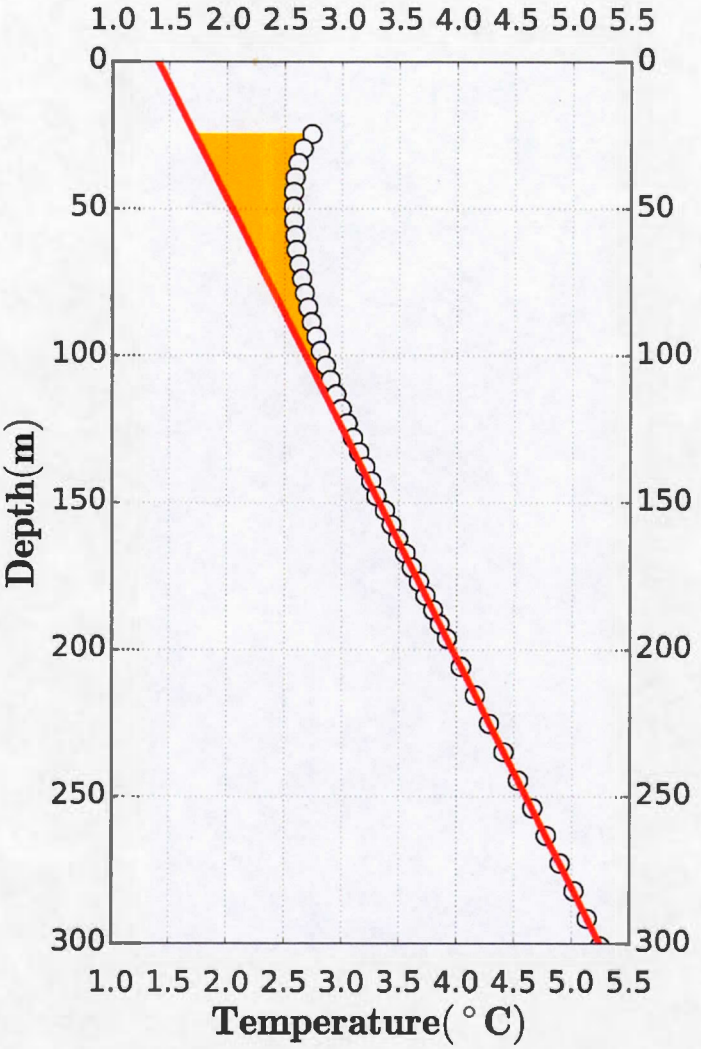

Figure 1.1 Borehole CA-9308. Borehole temperature profile, the dots are the temperature measurements $T(z)$, the red line is the fit, obtained by linear regression of the lower 100 meters, extrapolated to the surface $z = 0$ and the blue lines represent two maximum steady states related with the errors (in the intercept and slope) associated with the method to obtain the geothermal steady state $q_0 R(z) + T_0$. The reference temperature at the surface T_0 is associated to the intercept an the heat flux q_0 is related with the slope. The transient perturbation T_t (green area) related with the climate signal is obtained by the subtraction of the geothermal steady-state from the full profile.

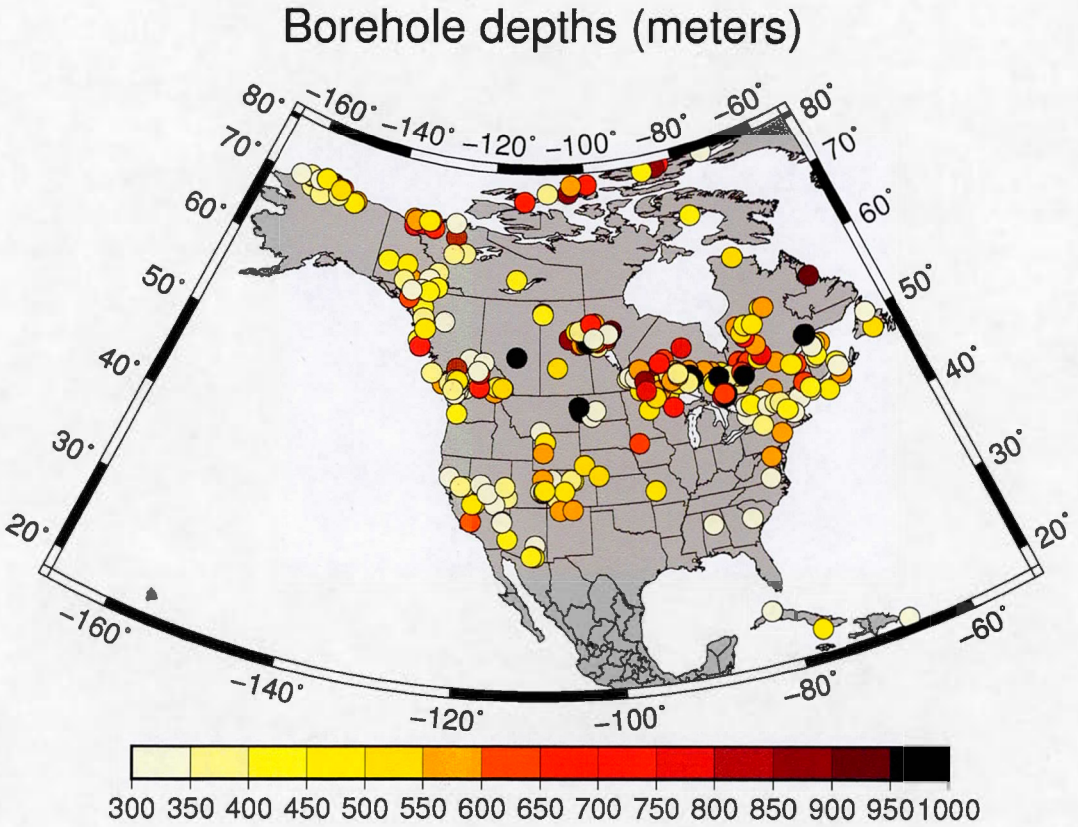

Figure 1.2 Location of the 510 selected boreholes. The colors represent the maximum depth of each borehole.

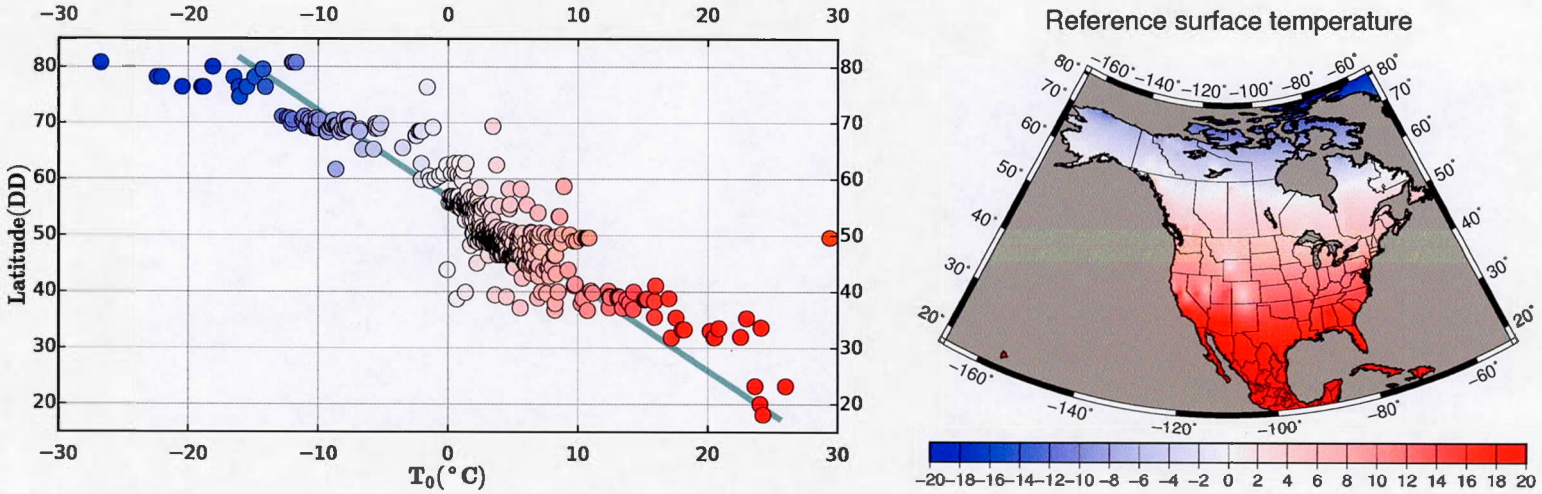

Figure 1.3 $T_0(°C)$ & Latitude relation. Left: Linear regression of T_0. The least square method fits with $R^2 = 83.1\%$. Right: Surface interpolation map of T_0 in degrees Celsius.

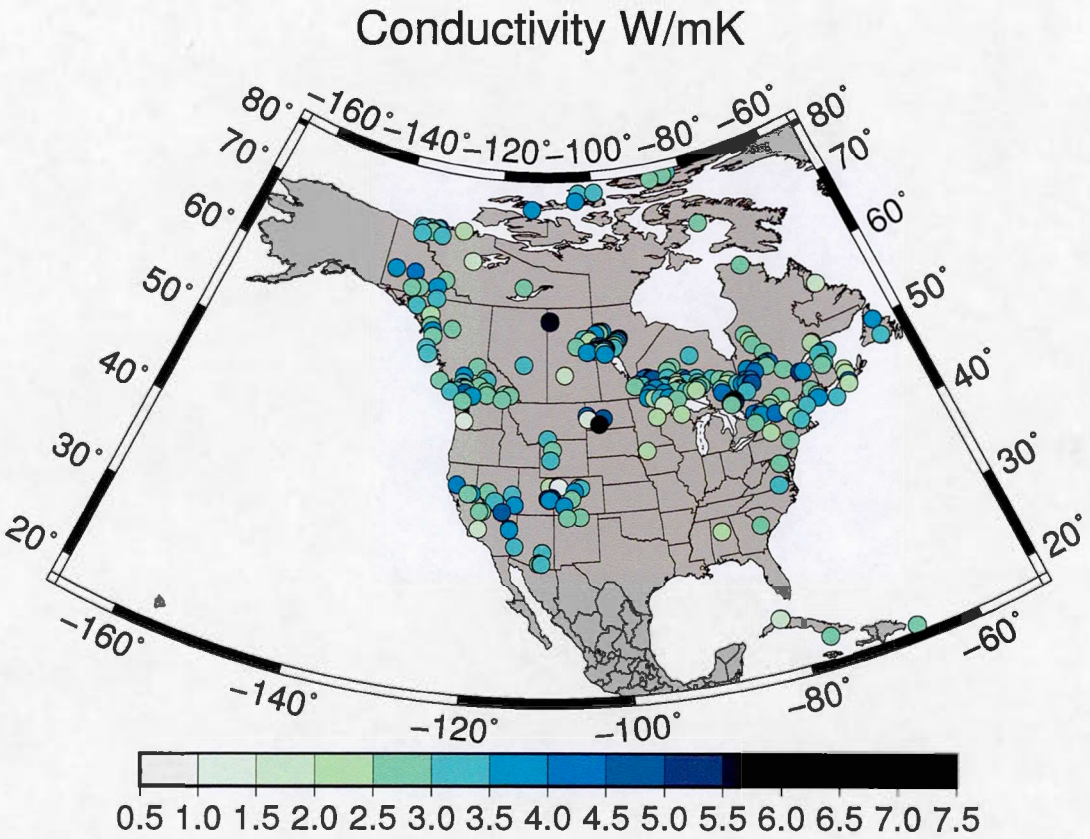

Figure 1.4 Conductivity of 453 boreholes. The colors represent the mean conductivity in each borehole.

CHAPTER II

NORTH AMERICAN REGIONAL CLIMATE RECONSTRUCTION FROM GROUND SURFACE TEMPERATURE HISTORIES

Fernando Jaume-Santero[1], Hugo Beltrami[2,3], Jean-Claude Mareschal[1]

[1]Centre de Recherche en Géochimie et en Géodynamique (GEOTOP), Université du Québec à Montréal, Montréal, Québec, Canada

[2]Climate & Atmospheric Sciences Institute and Department of Earth Sciences, St. Francis Xavier University, Antigonish, Nova Scotia, Canada

[3]Centre pour l'étude et la simulation du climat à l'échelle régionale (ESCER), Université du Québec à Montréal, Montréal, Québec, Canada

2.1 Abstract

Within the framework of the PAGES NAm2k project, 510 North American borehole temperature-depth profiles were analyzed to infer recent climate changes. To facilitate comparisons and to study the same time period, the profiles were truncated at 300 meters. Ground surface temperature histories for the last 500 years were obtained for a model describing temperature changes at the surface for several climate-differentiated regions in North America. The evaluation of the model is done by inversion of temperature perturbations using singular value decomposition and its solutions are assessed using a Monte-Carlo approach. The results within 95% confidence interval suggest a warming between 1.0 K to 2.5 K during the last two centuries. A regional analysis, composed of mean temperature changes over the last 500 years and geographical maps of ground surface temperatures, show that all regions experienced warming, but this warming is not spatially uniform and is more marked in northern regions.

2.2 Introduction

The energy imbalance between incoming and outgoing radiation in the upper atmosphere due to increased concentrations of greenhouse gases is well documented (e.g. Hansen *et al.*, 2011; von Schuckmann *et al.*, 2016). The redistribution of the excess energy between climate subsystems, the atmosphere, the oceans and the solid Earth, drives changes in global and regional scale climate. As the consequences of climate change are expected to be negative for natural ecosystems and society, it is necessary that the projected changes in climate be established with sufficient details and certainty to provide the framework for policy directives intended to mitigate, adapt and build resilience at the community scale. Although there are multiple measures of climate change, surface air temperature (SAT) is the most common indicator because of the availability of data over the

post-industrial period and also because it represents, in one way or another, the thermal conditions near the ground where people live.

The great majority of information on the future character and dynamics of the climate system comes from experiments with general circulation models (GCMs). GCMs are useful tools to assess future climate scenarios under different Representative Concentration Pathways (RCPs). However, because of the limited resolution of GCMs, many climatically relevant processes operating at less than the GCM grid size-scale are parameterized differently among model teams, such that GCM's simulations for the same RCP yield a climate state with a wide range of variability. Thus, GCM's simulations must be compared with data to assess the validity of their climate change projections (PAGES 2k-PMIP3 group, 2015; Smith *et al.*, 2015).

Since the availability of meteorological records is limited to the last 150 years, additional information can be obtained from climate-dependent natural phenomena to reconstruct long-term past climate changes (e.g. Masson-Delmotte *et al.*, 2013). Some of these indicators include data extracted from paleoclimate archives, such as ice cores (e.g. Oeschger and Langway, 1989; Bauer *et al.*, 2013; Thompson *et al.*, 2013), tree rings (e.g. Douglass, 1919; Briffa *et al.*, 1990; George and Ault, 2014), pollen (e.g. Davis *et al.*, 2003; Viau *et al.*, 2006, 2012; Jacques *et al.*, 2015) or geothermal data measured in boreholes (e.g. Mareschal and Beltrami, 1992; Bodri and Cermak, 2007; González-Rouco *et al.*, 2009).

However, these proxy indicators are responses to a complex dynamical system and do not represent a direct measure of climate variability. While they allow for the determination and comparison of past climate trends, each of these methods of paleoclimatic reconstruction has different resolution, advantages, disadvantages and uncertainties.

Furthermore, due to spatial and natural limitations, the significance of the global and regional climate reconstructions decreases as it extends back in time. Calibration disparities and different reconstruction methods among these proxies give rise to a diverse range of weaknesses and strengths, making each paleo-indicator better suitable for a specific timespan. From a large set of natural phenomena, those sensitive to temperature variations can be used as climate indicators to reproduce past temperature histories.

Collaborative efforts have been conducted under the '2k Network' of the Past Global Changes (PAGES) project to produce a global array of regional climate reconstructions for the past 2000 years using proxy data sets derived from different natural sources (2k Consortium, 2013). It is within this multidisciplinary framework that geothermal data measured in boreholes can contribute with low-frequency trends retrieved from anomalies of the underground thermal regime.

Temperature-depth profiles measured in boreholes have commonly been used to study the magnitude and spatial variability of the flow of heat from the interior of the Earth (Bullard, 1939; Benfield, 1939; Jaupart and Mareschal, 2015, and references therein). It has been known since the times of Fourier and Kelvin, that underground temperatures are affected by past surface conditions. Assuming a coupling between ground surface temperate (GST) and SAT, borehole temperature reconstructions can be used as climate indicators for hundreds to thousands of years before present. Lane (1923) and Hotchkiss and Ingersoll (1934) were the first to use temperature-depth profiles for paleoclimatic studies in an attempt to determine the timing of the last glacial retreat. It was only in the 1970s that studies to infer past climate from borehole temperature profiles (BTPs) became more systematic, developing into the field of borehole climatology (Cermak, 1971; Sass *et al.*, 1971; Beck, 1977).

Following the work of Lachenbruch and Marshall (1986), and because of concern about climate change, paleoclimatic reconstructions from borehole temperature data have become widespread, and have yielded local, regional, and global analyses (see Lewis, 1992; Bodri and Cermak, 2007; González-Rouco *et al.*, 2009). However, the majority of the data are from the northern hemisphere.

In North America, several for local and regional analyses have been performed (e.g. Beltrami and Mareschal, 1992; Guillou-Frottier *et al.*, 1998; Chouinard *et al.*, 2007). However, very few studies so far have addressed the entire North American continent.

In this paper, and within the framework of the PAGES NAm2k project, we aim to estimate regional trends in the GST change of the past 500 years in North America from a dataset containing almost twice the number of data and larger depth range ($> 300m$) than previous analyses. The dataset analyzed here contains 510 borehole temperature-depth profiles distributed over the North American continent.

2.3 Methodology

The thermal regime of Earth's subsurface is governed by the outflow of heat from the Earth's interior and by the temporal variations of the ground surface temperature. For a homogeneous subsurface with no internal heat sources and with no ground surface temperature variations, the temperature in the subsurface increases linearly with depth. This profile can be considered as in a quasi steady-state relative to the timescale of recent climatic variations, since it depends solely on heat flux from Earth's interior, which varies over much longer timescales. Persistent temporal changes in ground surface temperature propagate into the subsurface and are recorded as transient perturbations to this geothermal quasi steady-state. Because of heat diffusion, the amplitude of the subsurface

anomalies is proportional to the duration and magnitude of the ground surface temperature perturbations and decreases with time since their occurrence. Since these temperature fluctuations diffuse downward, only the low-frequency climate signals are preserved. To reconstruct the temporal evolution of the ground surface temperatures, the variation of the subsurface temperature as a function of depth is measured in boreholes following the procedure described in 2.3.7. The transient perturbation is then retrieved from the borehole temperature profile (BTP) and inverted as described in 2.3.3, to reconstruct the temporal ground surface temperature changes.

Furthermore, borehole climatology assumes that the ground surface temperature changes track long-term variations in surface air temperature. That is, it is assumed that ground surface and surface air temperature are coupled. This coupling has been confirmed by model simulations (e.g. González-Rouco *et al.*, 2006; García-García *et al.*, 2016), as well as data from continuous monitoring of air and ground temperature variations (Putnam and Chapman, 1996), and by comparing BTPs with meteorological records at nearby stations (Harris and Chapman, 1998b). However, the relationship between surface air temperature and ground surface temperature can also be altered by transients effects in the surface conditions such as land use and associated hydrological, snow and vegetation cover changes (Lewis and Wang, 1998; Gosselin and Mareschal, 2003b; Bartlett *et al.*, 2004). Thus, changes in ground surface temperature are not necessarily related to climate. Some of these perturbations of the surface environment can be observed at the time of measurement and should be considered prior to interpretation. When all non climatic effects have been ruled out, the interpretation of the perturbations of the temperature profiles allows us to reconstruct the past temperature changes at the surface.

2.3.1 Temperature-depth equation

In order to interpret the temperature depth profiles, we must be able to describe quantitatively the thermal regime of subsurface and also how it is affected by changes in surface temperature. This requires the solution of the heat diffusion equation for a continuous medium given by (Carslaw and Jaeger, 1959):

$$\frac{d}{dt}\left(\rho c_p T\right) - \vec{\nabla} \cdot \left(\lambda \vec{\nabla} T\right) = \dot{Q}_s \ , \tag{2.1}$$

where ρ is the density, c_p is the specific heat of the medium at constant pressure, λ is the thermal conductivity, $\vec{\nabla}$ is the vector differential operator and $\dot{Q}_s$ is the heat production rate per unit volume.

Because heat production rates in crustal rocks are small (on the order of 1 μW m^{-3}) and the effect of heat production is negligible for holes that are only a few hundred meters deep (< 1 mW m^{-2}), we have neglected heat production in this study.

Assuming that heat production can be neglected ($\dot{Q}_s \approx 0$), that there is no advection of heat $\left(\vec{v} \cdot \vec{\nabla} T = 0\right)$ and that Earth is interpreted as a homogeneous half-space, the temperature at a depth z is given by the superposition of the steady-state profile and the transient perturbation due to time variations of surface temperature:

$$T(z) = T_0 + q_0 R(z) + T_t(z) \ , \tag{2.2}$$

where T_0 is the long-term surface temperature, q_0 is the quasi steady-state heat flux and $R(z)$ is the thermal depth defined as (Bullard, 1939):

$$R(z) = \int_0^z \frac{dz'}{\lambda(z')} \ , \tag{2.3}$$

where $\lambda(z')$ is the thermal conductivity at depth z'. For constant conductivity, equation 2.2 is written as:

$$T(z) = T_0 + \Gamma_0 z + T_t(z) \ , \tag{2.4}$$

where $\Gamma_0 = q_0/\lambda$ is the quasi steady-state temperature gradient.

If thermal conductivity can be assumed constant for the measured depth interval ($\lambda(z) = \lambda$), the transient component of temperature is calculated from the one dimensional heat conduction equation (Carslaw and Jaeger, 1959).

$$\frac{\partial T}{\partial t} = \kappa \frac{\partial^2 T}{\partial z^2} \,, \tag{2.5}$$

where $\kappa = \frac{\lambda}{\rho c_p}$ is the thermal diffusivity, also assumed constant for all cases ($\kappa \approx 10^{-6}\mathrm{m}^2\ \mathrm{s}^{-1}$ or $\kappa \approx 31.6\mathrm{m}^2\mathrm{y}^{-1}$). The main reason to use an average value is because thermal diffusivity measurements were not made on rock samples for most of the boreholes. Equation (2.5) must be solved with initial and boundary conditions: the temperature perturbation at the surface, $T(z = 0, t) = T_0(t)$, no perturbation for $z \to \infty$, $T(z = \infty, t) = 0$, and $T(z, t = 0) = 0$. The use of the one dimensional equation (2.5) is valid if the surface temperature variations have much larger spatial scale than their penetration depth (Clauser and Mareschal, 1995). Equation (2.5) also shows that the diffusivity determines the scaling relationship between time τ and depth L, scaling as $\tau \propto L^2/\kappa$. Periodic surface temperature variations propagate as a damped wave with skin depth $\delta = \sqrt{\kappa T/\pi}$ (Jaupart and Mareschal, 2011). For standard values of κ for rocks, the amplitude of the wave associated with the annual temperature cycle is 10% of its surface value at 10m depth. For 100 year and 1000 year cycles, the amplitude of the wave is 10% its surface value at 100 and 300m respectively.

2.3.2 Parametrization of the temperature anomaly

Assuming that Earth's underground thermal regime is at equilibrium and there are negligible diffusivity (κ) changes in the subsurface, the transient perturbation temperature $T_t(z) = T(z, t = 0)$ defined over a semi-infinite half-space with surface temperature $T(z = 0, t) = T_0(t)$ at time t before present is given by (Carslaw

and Jaeger, 1959)

$$T_t(z) = \int_0^\infty \frac{z}{2\sqrt{\pi\kappa t}} \exp\left(\frac{-z^2}{4\kappa t}\right) T_0(t) t^{-\frac{3}{2}}\, dt \ . \tag{2.6}$$

For an instantaneous temperature change ΔT at time t before present, integrating the equation (2.6) yields (Carslaw and Jaeger, 1959)

$$T_t(z) = \Delta T \ \mathrm{erfc}\left(\frac{z}{2\sqrt{\kappa t}}\right) , \tag{2.7}$$

where erfc is the complementary error function:

$$\mathrm{erfc}(x) = 1 - \mathrm{erf}(x) = 1 - \frac{2}{\sqrt{\pi}} \int_0^x \exp(-u^2) du \ . \tag{2.8}$$

In order to approximate ground surface temperature changes, we assume that ground surface temperature can be replaced by its average value over time intervals of several years, so that the daily, annual, and solar activity cycles are removed.

Defining the ground temperature changes as ΔT_k during K time steps (i.e. ΔT_k for $t_{k-1} < t < t_k$ where $k = 1, ..., K$), the transient perturbation is the sum of the contributions for each time step:

$$T_t(z) = \sum_{k=1}^{K} \Delta T_k \left[\mathrm{erfc}\left(\frac{z}{2\sqrt{\kappa t_k}}\right) - \mathrm{erfc}\left(\frac{z}{2\sqrt{\kappa t_{k-1}}}\right)\right] \ . \tag{2.9}$$

Equation (2.9) gives the temperature anomaly $T_t(z)$ due to a sequence of ground surface temperature changes ΔT_k for K time intervals. The problem consists in determining the ground surface temperature history from the temperature versus depth anomaly, $T_t(z)$, at a given site. This is routinely done using inversion techniques.

2.3.3 Inversion

Combination of equations (2.2) and (2.9) yields a linear equation with the parameters T_0, Γ_0, and ΔT_k for each depth with temperature data. Thus, the

inversion consists of solving the resulting system of linear equations. Obtaining the solution, however, is never straightforward because the system is "ill-conditioned", i.e., its solution is unstable (a small change in the data causes a very large change in the solution) and, for all practical purposes, the solution is non-unique. Different methods have been developed to solve inverse problems: the Backus-Gilbert method (Parker, 1977, 1994), singular value decomposition (SVD) (Lanczos, 1961; Jackson, 1972), Bayesian inversion (Tarantola and Valette, 1982), Tikhonov regularization (Tikhonov and Arsenin, 1977), and Monte-Carlo simulations (Mosegaard and Tarantola, 1995). One of the first applications of inversion to borehole temperature data was based on the Backus-Gilbert method (Vasseur *et al.*, 1983); Shen and Beck (1991) proposed an algorithm based on the Bayesian approach while Mareschal and Beltrami (1992) used singular value decomposition. Because of the very small number of parameters, these methods of inversion are not computationally intensive. The Monte-Carlo method, which has been used by Mareschal *et al.* (1999) and Kukkonen and Jõeleht (2003), explore the entire parameter space and requires larger computational resources than the other methods. In this study, we have used singular value decomposition to find the ground surface temperature history because of its simplicity and then used a Monte-Carlo procedure to determine the range of model parameters that satisfy the data within some error bounds.

2.3.4 Subsurface temperature anomaly

In this study we determined the long-term surface temperature and quasi steady-state geothermal gradient by linear regression to the lowermost 100 meters of the measured temperature profile. This linear regression represents the geothermal quasi steady-state (eq. 2.2) from which the subsurface temperature anomalies are estimated. The anomaly $T_t(z)$ is obtained by subtracting this quasi-equilibrium thermal profile from the measured temperature profile. The least square regression

also yields an estimate of the maximum error on slope and intercept estimates (95% confidence interval). These error bounds represent the upper and lower limits for the quasi steady-state temperature profile, hereafter referred to as the extremal geothermal steady-states. Figure 2.1 shows an example of a measured temperature profile and its estimate subsurface temperature anomaly, near Lynn Lake, Manitoba.

2.3.5 Singular value decomposition

After removal of the quasi steady-state component of the temperature profile, we are left with a system of linear equations between J temperature anomalies $T_t(z_j) = T'_j$ for each depth and the K parameters of the surface temperature history ΔT_k:

$$\begin{pmatrix} T'_1 \\ \vdots \\ T'_j \\ \vdots \\ T'_J \end{pmatrix} = \begin{pmatrix} A_{11} & \cdots & A_{1k} & \cdots & A_{1K} \\ \vdots & \ddots & \vdots & \ddots & \vdots \\ A_{j1} & \cdots & A_{jk} & \cdots & A_{jK} \\ \vdots & \ddots & \vdots & \ddots & \vdots \\ A_{J1} & \cdots & A_{Jk} & \cdots & A_{JK} \end{pmatrix} \begin{pmatrix} \Delta T_1 \\ \vdots \\ \Delta T_k \\ \vdots \\ \Delta T_K \end{pmatrix}, \tag{2.10}$$

where the A_{jk} are given by equation 2.9

$$A_{jk} = \operatorname{erfc}\left(\frac{z_j}{2\sqrt{\kappa t_k}}\right) - \operatorname{erfc}\left(\frac{z_j}{2\sqrt{\kappa t_{k-1}}}\right). \tag{2.11}$$

The number of equations J could be greater, equal, or less than the number of parameters K. In general, this number is larger than the number of parameters, but this does not ensure that the system 2.10 has a unique solution.

Writing formally, the matrix of equation (2.10)

$$\boldsymbol{\Theta} = \mathbf{A}\mathbf{x} \tag{2.12}$$

where $\mathbf{\Theta}$ is the data vector, $\mathbf{A}$ is the rectangular $(J \times K)$ matrix containing the coefficients of the equations, and $\mathbf{x}$ is the vector of unknown coefficients.

SVD decomposes the matrix as (Lanczos, 1961):

$$\mathbf{A} = \mathbf{U}\mathbf{\Lambda}\mathbf{V}^{\top} \tag{2.13}$$

where $\mathbf{U}$ is an $(J \times J)$ orthonormal matrix in data space, $\mathbf{V}$ is an $(K \times K)$ orthonormal matrix in parameter space and $\mathbf{\Lambda}$ is a $J \times K$ rectangular matrix with only non-zero values, called "singular values" λ_l $(l = 1, ..L)$ on the diagonal, with $L \leq \min(J, K)$. The singular values are the square root of the eigenvalues of the $J \times J$ symmetric matrix $(\mathbf{A}^{\top}\mathbf{A})$. If $L < J$, the system is overdetermined and if $L < K$, it is underdetermined. Whether the system is overdetermined, underdetermined, or both, it admits a generalized solution given by:

$$\mathbf{X} = \mathbf{V}\mathbf{\Lambda}^{-1}\mathbf{U}^{\top}\mathbf{\Theta} \tag{2.14}$$

where Λ^{-1} is a $K \times J$ rectangular matrix with L elements $\frac{1}{\lambda_l}$ on the diagonal completed with zeros. This provides a solution which is usually not very meaningful (Mareschal and Beltrami, 1992) because it is unstable and dominated by noise. The instability of the solution comes the presence of very small singular values λ_l. In the case of borehole temperature profiles, the fifth largest singular value is 0.01 times the largest one, and the tenth is $< 10^{-8}$ times the largest one, that is, less than numerical noise. In order to stabilize the solution, we eliminate the part associated to the very small singular values. This is done by replacing with 0 the inverse of all the singular values less than a "*cut-off value*", typically on the order of 10^{-2}. This means that the solution is obtained as a linear combination of 4 orthogonal vectors in parameter space. Each vector represents a surface temperature history, and the vectors selected are those that have the largest impact on the data. By eliminating the small singular values, we choose to neglect the part of the solution that has little or no effect on the data, and therefore cannot be

determined. In general, the selection of a cutoff value is done by trial and error, by increasing the number of singular values and inspecting the solution for signs of instabilities and loss of resolution, i.e. large non physically meaningful fluctuations or no useful information. For this study, we used a cut-off of 0.03 which resulted in 4 singular values being retained for all profiles except for CU-C-357 measured in Cuba, where only 3 singular values were retained.

The choice of a proper parametrization is useful to reduce the number of parameters to be estimated. This can be achieved by increasing the duration of the ground surface temperature history model time intervals. For very long reconstructions a logarithmic distribution has been used (e.g. Mareschal *et al.*, 1999). For the present study, we have used a model consisting of a series of 10 time intervals of varying duration after testing with different parametrizations and verified that similar results were obtained (see Appendix 1). Their temporal length is smaller for the near (past 100 years) than for the remote past. The distribution used here is:

$$t_k = \{0,\ 25,\ 50,\ 75,\ 100,\ 150,\ 200,\ 250,\ 300,\ 400,\ 500\} \tag{2.15}$$

When doing regional averages, the GST histories are shifted in time to account for the date when they were logged (i.e. years before present is the year of measurement).

As an example, Figure 2.2 shows the result of inversion of the subsurface temperature anomaly for the Fox mine site, and the results from the inversions of the two extremal geothermal steady-states.

2.3.6 Forward model

GST histories can be forward-modelled using equation (2.9) to assess the fit of the SVD inversion with respect the initial anomaly profile. A Monte-Carlo procedure

was applied (Mareschal *et al.*, 1999; Kukkonen and Jõeleht, 2003; Chouinard *et al.*, 2007) by randomly perturbing the model parameters to find the range of GST histories that fit the data within a maximum root mean square (RMS) error less or equal than the difference between the forward-modelled SVD reconstruction and the anomaly. Using the Monte-Carlo approach to invert the temperature profiles is particularly inefficient because it requires a very large number of simulations to explore the entire parameter space. It requires at least $10^7 - 10^8$ longer computational time than using the SVD inversion. However, this can be alleviated by using a-priori information or the result of an existing ground surface temperature history from inversion to reduce the region explored in parameter space. After the Monte-Carlo inversion, the mean and standard deviation of all the accepted models are estimated to show the trend of all the solutions with a same or better fit than the inversion for 4 singular values. For the present study, we halted the calculations after 500 models are accepted or after 5 million forward model comparisons.

This is illustrated in Figure 2.3 that shows the results of the Monte-Carlo inversion for the Fox mine temperature profile.

2.3.7 Data

We have compiled from different sources (Table B.1) a set of temperature depth profiles for North America. Thousands of borehole temperature profiles have been measured in North America, but the majority of them are not suitable for climate reconstructions. For instance, bottom hole temperatures, commonly measured during oil exploration drilling, are not measured at equilibrium, and are affected by errors several times larger than the signals we want to detect. Water wells are usually too shallow to be useful and likely to be affected by water flow. Many holes were drilled for geothermal energy in the western US but are often perturbed by

water circulation. For heat flow or climate studies, the most useful boreholes are those that have been drilled by mining companies for exploration or development purposes. Oil exploration wells cannot be used for several reasons: holes that are not put in production must be cemented and they are not accessible for steady-state measurements. In addition, oil-exploration boreholes have a large diameter and are susceptible to perturbations due to convection in the hole. Furthermore, sedimentary rocks are permeable and often affected by convection as well. Hence, their temperature profiles are not suitable for climate studies. Drilling perturbs the thermal regime of the subsurface around the drill site and some time is needed for thermal re-equilibration. As a rule of thumb, the time to return to equilibrium is $\sim$ 5-6 times the duration of drilling. The temperature in the hole is measured with a calibrated thermistor. The probe is lowered in the hole and measurements are made at fixed intervals along the length of the hole, which results in varying depth intervals as most boreholes are inclined. The sampling interval is usually 10m, sometimes 50 feet for US and old Canadian temperature logs. Continuous measurements can be obtained, but are not common because they require heavy equipment. Measurements made above the water table are rarely equilibrated; consequently, the upper 20 or 30m of the temperature logs must be discarded. This is also done in order to eliminate the annual temperature variation signal. In heat flow studies, core samples must be obtained to determine the underlying rock's thermal conductivity and heat production. Changes in thermal conductivity are thus included in the interpretation of these data.

2.3.8 Data selection

Different criteria have been applied in selecting the temperature profiles. Temperature profiles must be at least 300 meters deep to contain the signal to allow for the reconstruction of the climate of the past 500 years. Profiles must include at least 10 measurements, and must include measurements in the uppermost 100m.

Profiles that meet these conditions are then visually inspected to detect discontinuities, signs of water flow, or other perturbations that make them unsuitable for interpretation. The vertical temperature gradient profile amplifies the noise and usually provides a better diagnostic for the level of noise in the measurements. Although we have not established a quantitative criterion for selecting profiles based on the noise level, we have examined the vertical gradients to eliminate obviously unsuitable profiles.

After selection process, we retained 510 profiles. These data will be available in a public database in Figshare (Jaume-Santero *et al.*, 2016). Borehole locations are not uniformly distributed across the continent (Figure 2.4). Several regions are very poorly sampled because they are very difficult to access (Alaska and most of Canada, north of 56 °). Furthermore, in the northernmost regions, drill holes cannot be routinely logged because of permafrost. Temperature logging in frozen ground requires special equipment to be emplaced at the end of drilling and is very costly. The southern part of the Canadian Shield is the region most extensively sampled because of the mining activity and because the temperature profiles are less likely to be perturbed in the crystalline rocks of the Shield. In contrast, numerous drill holes are available in the south-western US, but most of them cannot be used because they are perturbed by water flow. The sedimentary cover in many regions of the US explains that no suitable holes have been found for many states, including Texas and Oklahoma and the south-eastern US. This very uneven distribution of suitable boreholes is demonstrated in Table 2.2 which shows the number of temperature profiles for each one of the regions defined for Pages2k (McKay, 2014).

2.4 Results & discussion

All 510 borehole temperature-depth profiles were inverted individually to reconstruct the GST histories for the past 500 years. The model consisted of a series of 10 temperature change intervals of varying temporal duration following the distribution (2.15). For the inversion, we used the singular value decomposition inversion with a cutoff of 0.03, retaining 4 singular values. We also used the Monte Carlo methodology to estimate the range of parameter values consistent with the data. The means of the GST's obtained by Monte-Carlo are similar to the solution by SVD inversion. With the condition that the RMS difference between model and data be no larger than the misfit for the SVD, the 2σ range of accepted models is no larger than 0.44 K.

2.4.1 North-American ground surface temperature change

We have calculated the variation in ground surface temperature for North America by averaging all the Monte-Carlo inversions. The averaging was done on a yearly basis because the logging dates vary between boreholes from 1958 to 2014 (Figure 2.5).

Figure 2.5 shows the individual Monte-Carlo inversions together with their average. This result seems consistent because similar mean North American GST histories were obtained from different parametrizations (see Appendix 1). However, individual inversions in Figure 2.5 exhibit a wide variability due to the large range of latitudes ($\sim 80°N$ to $\sim 18°N$) in the data set of GST reconstructions.

Nevertheless, a clear warming transition is observed from the pre-industrial era (1500-1800) to the post-industrial era (1800-2000). The temperature difference between the pre-industrial mean (1500-1700) and the mean between the years (1961-1990) is 1.1 K. Because of the marked warming of the past 50 years, the

total change of the average ground surface temperature is 1.8 K between pre-industrial time and the year 2000.

These results agree with findings of other ground surface temperature reconstructions (Huang *et al.*, 2000; Harris and Chapman, 2001; Beltrami and Bourlon, 2004; Pollack and Smerdon, 2004). Furthermore they agree with instrumental data, CRUTEM4 (Jones *et al.*, 2012; Morice *et al.*, 2012), pollen and tree ring reconstructions (2k Consortium, 2013; Trouet *et al.*, 2013). All of them presented as departures from the 1904-1980 temperature mean (Figure 2.6). However, the reconstructed GST warming signal for the past 200 years is greater than results from pollen reconstructions, being consistent with findings of PAGES 2k-PMIP3 group (2015). Furthermore, multi-centennial temperature reconstructions for North America and the Northern Hemisphere, based on multiproxy records, showed trends similar to temperature-depth reconstructions: an unclear cold-warm trend followed by a clear increase in temperature for the past two centuries (Moberg *et al.*, 2005; Mann *et al.*, 2008; PAGES 2k-PMIP3 group, 2015). This warming has also been recorded by instrumental data for the last century (Hansen *et al.*, 2010). However, the difference between the long-term pre-industrial temperature mean and the recent past trend is larger in the ground surface temperature histories than in the pollen-based and tree-ring reconstructions. These disparities among different proxy-based reconstructions can be attributed to a combination of factors as discussed in Pollack and Smerdon (2004). For instance, while a significant part of boreholes are located in higher latitudes (Eastern & Central Canada), tree-ring data are mainly obtained in lower latitudes (Western US). Therefore, the spatial distribution of proxies could explain colder temperatures. Other possible reasons for those differences are the seasonal bias of the proxies and the limitation of borehole climatology in resolving short-term variability.

The Little Ice Age (LIA) is not resolved because the boreholes were truncated

at 300 meters which is too shallow to allow for a clear LIA signal in most of the borehole profiles as can be shown with synthetic models (Mareschal and Beltrami, 1992) and was confirmed in several studies (Guillou-Frottier *et al.*, 1998; Chouinard *et al.*, 2007; Pickler *et al.*, 2016a). Some profiles, such as the Fox Mine shown in Figure 2.2, may indeed show the LIA cooling, but the majority of them do not. In addition, because the LIA signal may vary both in time and in amplitude between regions, a marked signal cannot be expected from averaging weak and inconsistent signals.

2.4.2 Regional averages

The PAGES NAm2k working group divided the North American continent into seven subregions for paleoclimate studies (McKay, 2014). The distribution of boreholes between these regions is extremely uneven as shown in Table 2.2, with only 4 regions appearing adequately sampled (Central & Eastern Canada, Midwestern US, Arctic, and Pacific Northwest). Furthermore, the sampling in the Arctic and the Pacific northwest is very biased because all the boreholes are close to the coast (Figure 2.4). For the three other regions, the sampling is insufficient to obtain robust climate trends.

A warming by $\sim$1.8 K for the past 200 years is observed in the Arctic (Figure 2.7a), but the histories show wide variability. This variability suggests the need for smaller-scale regional analysis such as the pollen-based reconstructions of Gajewski (2015) and Viau and Gajewski (2009). Their findings illustrate that recent Arctic increases in temperature have exceeded natural climate variability, which is consistent with borehole GST reconstructions.

The region of the Pacific northwest (Western Canada & Northwestern US) shows an increase in temperature of $\sim$0.8 K with a 95% variability range of $\sim$3.4 K for the last two centuries(Figure 2.7b). This warming is consistent with previous

findings (Majorowicz and Safanda, 2001).

An average warming of ~1.1 K with a 95% variability range of ~2.2 K, for the past two centuries is observed for Central & Eastern Canada (Figure 2.7c), agreeing with previous studies (Beltrami *et al.*, 1992; Guillou-Frottier *et al.*, 1998).

The Western US GST mean shows a small increase in temperature of ~0.2 K ± 1.8 K (Figure 2.7d). This could be the result of strong irrigation processes and water flow at the sampling locations, but the number of borehole temperature profiles available in the region are insufficient to verify this. The limited amount of useful borehole temperature profiles for Western US (only 9) were logged in the 1960's, the most recent of them was measured in 1970. Thus, it is not possible to reconstruct the past 40 years when the increase in temperature recorded in weather stations was more marked.

The average reconstruction for the Midwestern US suggests a warming of ~1.3 K ± 2.0 K for the last 50 year average (Figure 2.7f). This recent warming has also been observed in previous GST reconstructions as well as SAT records (Skinner and Majorowicz, 1999) and could reflect the significant land use change in the region.

A warming of ~1.0 K ± 1.0 K has been reconstructed for the last 200 years in the Eastern United States (Figure 2.7e). However, due to the rejection of borehole profiles affected by topography and water flow, the number of reconstructions made is too small to describe with confidence climate trends of the region.

There is a warming trend of ~3.0 K ± 3.6 K until the mid 1960s in the Caribbean (Figure 2.7g). Due to the low number of profiles sampled in Mexico (0) & the Caribbean (4), it is not possible to obtain a robust reconstruction for this region.

2.4.3 Geographical representation

A North American regional analysis of GST changes is presented as six geographical maps for different 50-year time intervals during the last 300 years, (Figure 2.8).

Trends prior to 1681 are not shown because they did not yield significant information. However, a small (~0.5 K) cooling is observed in certain regions. Previous small scale regional analyses have reconstructed a LIA signal during this period (e.g. Beltrami and Mareschal, 1992; Chouinard *et al.*, 2007). Furthermore, the regional variability of the cooling is consistent with previous studies, illustrating that not all regions of North America present a LIA signal (Gosselin and Mareschal, 2003a; Mann *et al.*, 2009). However, due to the truncation at 300m of the temperature-depth profiles analyzed here, a clear LIA signal cannot be resolved.

Figure 2.8 indicates a warming trend of $\sim$ 1-2 K in most parts of North America during the last 200 years. This is consistent with previous studies (Huang *et al.*, 2000; Harris and Chapman, 2001; Beltrami *et al.*, 2003). A cooling trend is observed in central California. Stevens *et al.* (2008) shows how this differs from the output of the ECHO-G model and postulates that it is the result of intensive irrigation in California's central valley, which could drive a regional cooling signal (Kueppers *et al.*, 2007). A similar cooling signal is observed in British Columbia which might be associated with irrigation in the Fraser Valley. On the Canadian east coast, Newfoundland presents little to no changes with respect the long-term mean. This agrees with meteorological data for the region (Gullett and Skinner, 1992). The absence of temperature profiles along the Gulf coast and Mexico does not allow for any determination of climate trends. The southwestern US is also a region where the number of boreholes is not enough for reliable reconstructions.

For these regions, multi-proxy approach would be necessary to improve the reconstruction of regional past climate in regions with an insufficient number of borehole profiles.

2.5 Conclusions

The average North American ground surface temperature change reconstructed from 510 boreholes deeper than 300 meters, suggests a warming of ~1.8 K for the last 200 years. However, these temperatures exhibit a wide range of spatial variability among all regions. For instance, reconstructed regional ground surface temperature changes for seven climate distinct regions, defined within the PAGES NAm2k project, suggest a warming range of ~0.5 K to ~2.0 K with a variability 2σ, no smaller than 1.0 K. Furthermore, regional variations of GST yield a warming range of 1 K to 2 K between 1780 and 1980. These warming trends are consistent with multi-proxy reconstructions.

Although the number of borehole temperature profiles for North America has been notably increased in our study, it is still insufficient to guarantee a non spatial-biased regional analysis because their distribution is not sufficiently uniform. Nevertheless, despite spatial and natural limitations, subsurface thermal profiles obtained from boreholes provide robust long-term GST histories which could be used to improve climate multi-proxy-based reconstructions. Those enhanced reconstructions would bring out worthwhile information for a straightforward assessment of past climate GCM outputs.

2.6 Appendix 1

In this appendix, we have assessed the consistency of the results obtained for several time parametrizations and different methods used to obtain the geothermal steady-state. In borehole climatology, two distinct methods can be used to deter-

mine the geothermal "quasi" steady-state: (1) calculating linear regression of the lowermost 100 meters (Beltrami *et al.*, 2011, 2015) and (2) including T_0 and Γ_0 into the parameter vector and solving the system of equations using the full profile (Pickler *et al.*, 2016b). The first method was utilized in this study. However, a validation test was run to ensure that both methods produced consistent results. The full profile method yielded mean temperatures similar to those calculated using the linear regression (Figure 2.9). The main difference in the individual inversion consisted in a smaller deviation of the reconstructed temperatures and a smaller jump at the start of the ground surface temperature history.

Another validation test was performed to ensure that the number and distribution of the time-steps did not significantly affect the mean ground surface temperatures. Increasing the number of time-steps from 10 to 25 in the inversion reconstructed similar mean temperature trends. Furthermore, an inversion utilizing equal length time-steps was compared with the ones presented in the results, which use time-steps of varying length. Both methods gave similar results.

These validation tests demonstrate the consistency of our results and the robustness of our reconstructions when utilizing various parametrizations.

2.7 Acknowledgements

We acknowledge the work of many researchers in the last half century who have contributed data to the borehole climate community and that are included in this work. This study was undertaken as part of the Past Global Changes (PAGES) project, which in turn received support from the US and Swiss National Science Foundations. Special thanks to William D. Gosnold for providing information about Midwestern boreholes and Jason E. Smerdon for suggesting this collaboration. This work was supported by grants from the Natural Sciences and Engineering Research Council of Canada Discovery grant (NSERC DG 140576948) and the Canada Research Program (CRC 230687) to H. Beltrami. Computational facilities were provided by the Atlantic Computational Excellence Network (ACEnet-Compute Canada) with support from the Canadian Foundation for Innovation. H. Beltrami holds a Canada Research Chair in Climate Dynamics. FJS and CP are funded by graduate fellowships from a NSERC-CREATE Training Program in Climate Sciences based at St. Francis Xavier University.

Table 2.1 Recorders useful for temperature histories. It presents their minimum resolution and maximum time range of reconstruction.

Archive	**Resolution**	**Range (yrs)**
Satellites & stations	hourly	$\sim 10^2$
Historical data	daily/seasonal	$\sim 10^3$
Tree rings	seasonal	$\sim 10^4$
Ice cores	annual	$> 10^5$
Pollen	decadal	$\sim 10^5$
Boreholes	decadal/centennial	$\sim 10^5$

Table 2.2 Distribution of borehole between regions as defined for PAGES2k McKay (2014).

Region	Number of profiles
Arctic	78
Pacific NW	78
Central & Eastern Canada	220
Western US	21
Eastern US	9
Midwestern US	100
Caribean	4

Table 2.3 Data sources where the temperature-depth profiles were taken.

Source name	Availability
University of Michigan	`http://www.earth.lsa.umich.edu/`
SMU Geothermal Lab	`http://geothermal.smu.edu/`
GEOTOP database	`http://www.geotop.ca/`
NOAA borehole datasets	Huang *et al.* (1999)
USGS array	`www.aoncadis.org/dataset/USGS_DOI_GTN-P/`
Canadian geothermal data compilation	Alan M. Jessop et al.
Jean-Claude Mareschal's data book	Jean-Claude Mareschal
Richard Scattolini, Ph.D. thesis Scattolini (1978)	

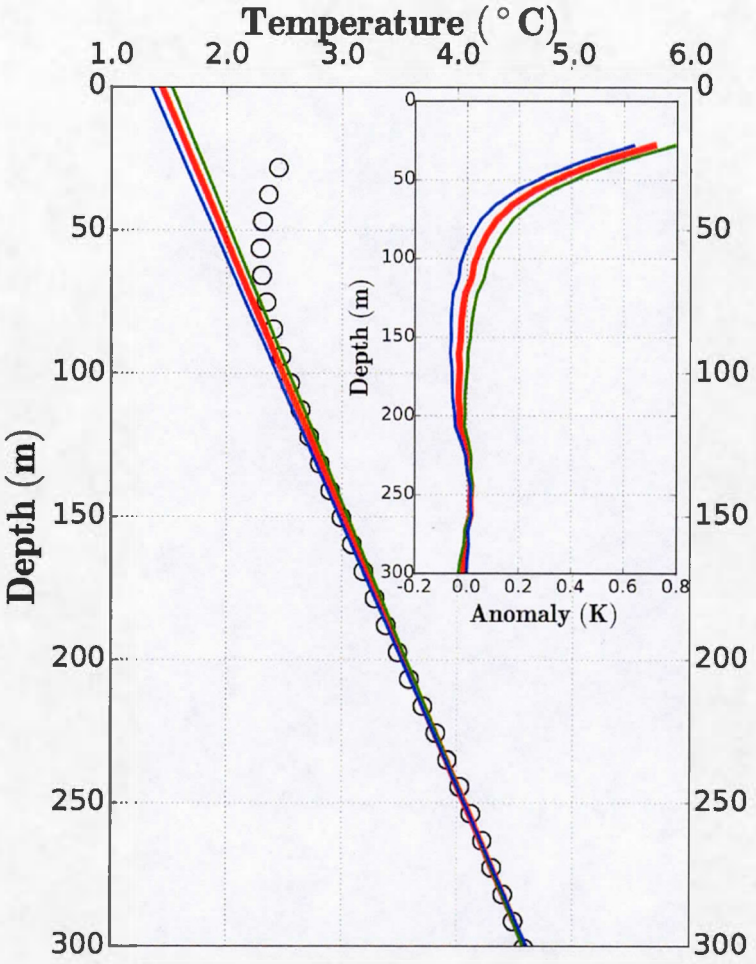

Figure 2.1 Temperature profile measured at Fox Mine (CA-9519), Lynn Lake, northern Manitoba, Canada. Main panel: Measurements are shown in circles $T(z)$, the red line represents the geothermal steady-state, obtained by linear regression of the lowermost 100 meters, and extrapolated to the surface ($z = 0$). Blue and green lines represent the 95% confidence interval from the linear regression. Inset: Transient perturbation or anomaly relative to the geothermal steady-state (red line) and the 95% confidence interval (blue and green lines). For this site, the geothermal steady-state is given by $\Gamma_o z + T_0 = (10.51 \frac{K}{km} \pm 0.34 \frac{K}{km}) \times z + (1.44°C \pm 0.19°C)$ (z in km).

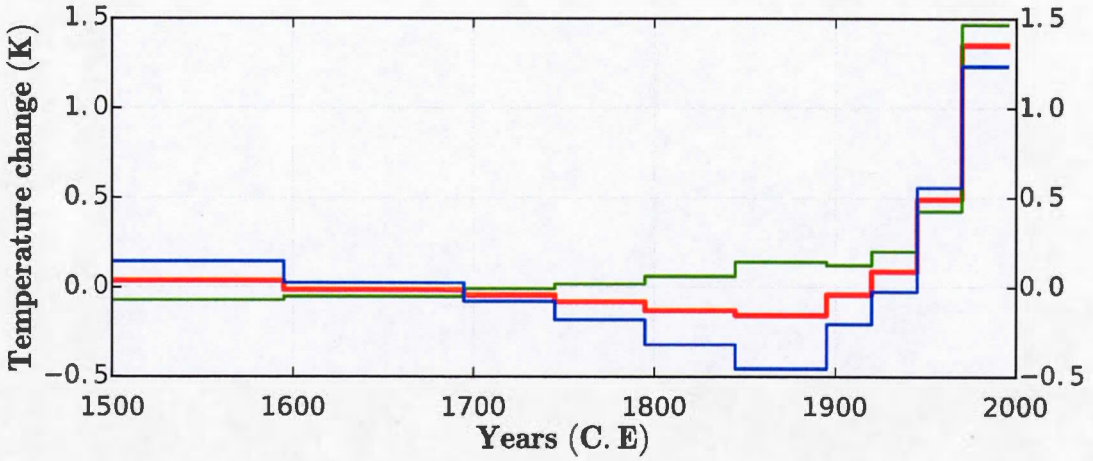

Figure 2.2 Ground surface temperature history for CA-9519 (Fox Mine, 1995). The red line represents the ground surface temperature history reconstructed from inversion. The blue and green lines are the GSTs for the anomalies estimated from the 95% uncertainty limits of the quasi steady-state profile.

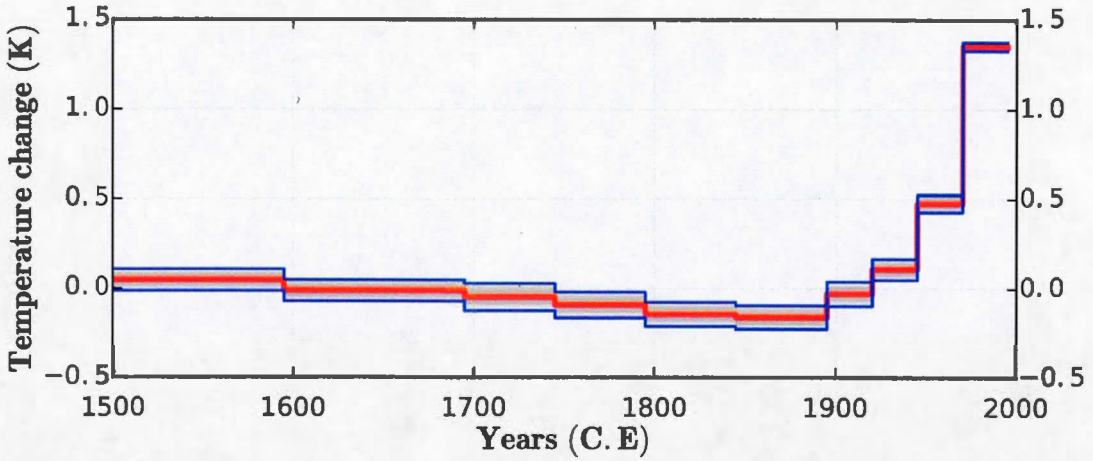

Figure 2.3 CA-9519 (Fox Mine, 1995) Mean ground surface temperature history (red) and 2σ uncertainty intervals (blue) from the Monte-Carlo inversion. The grey lines represent all the perturbed models within an interval determined by the RMS misfit from the SVD inversion.

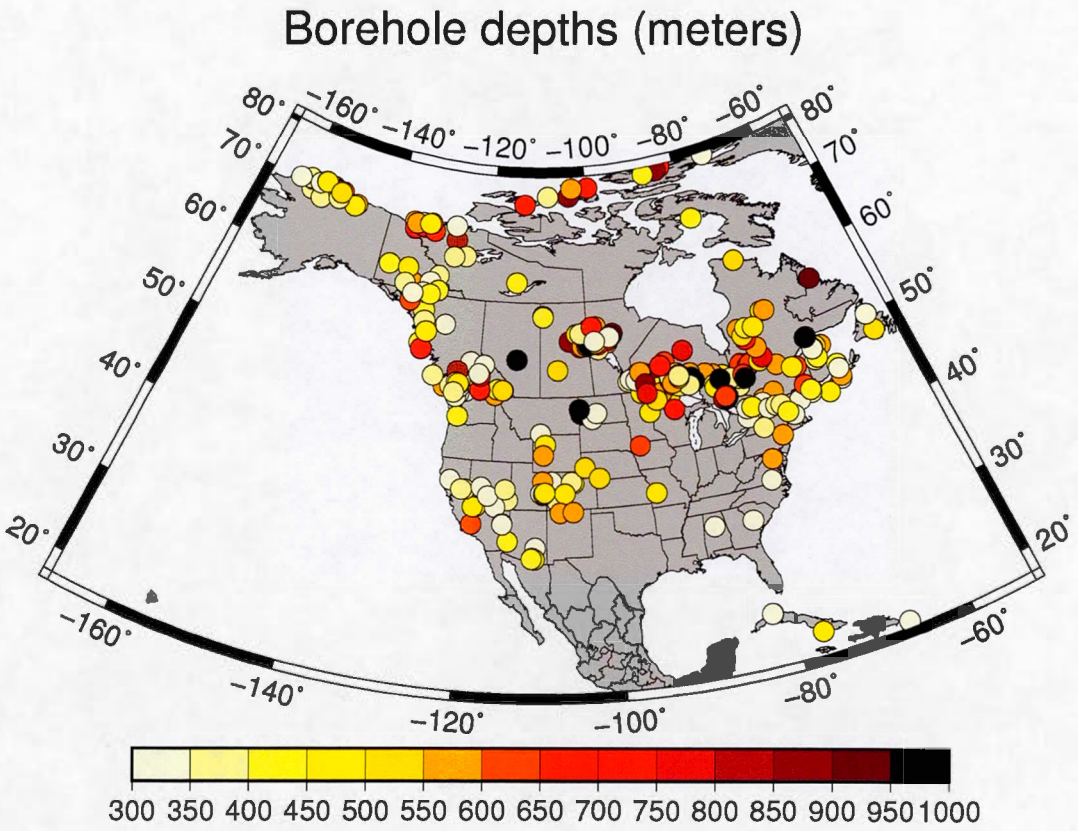

Figure 2.4 Location of the 510 selected boreholes. The colors represent the maximum depth of each borehole.

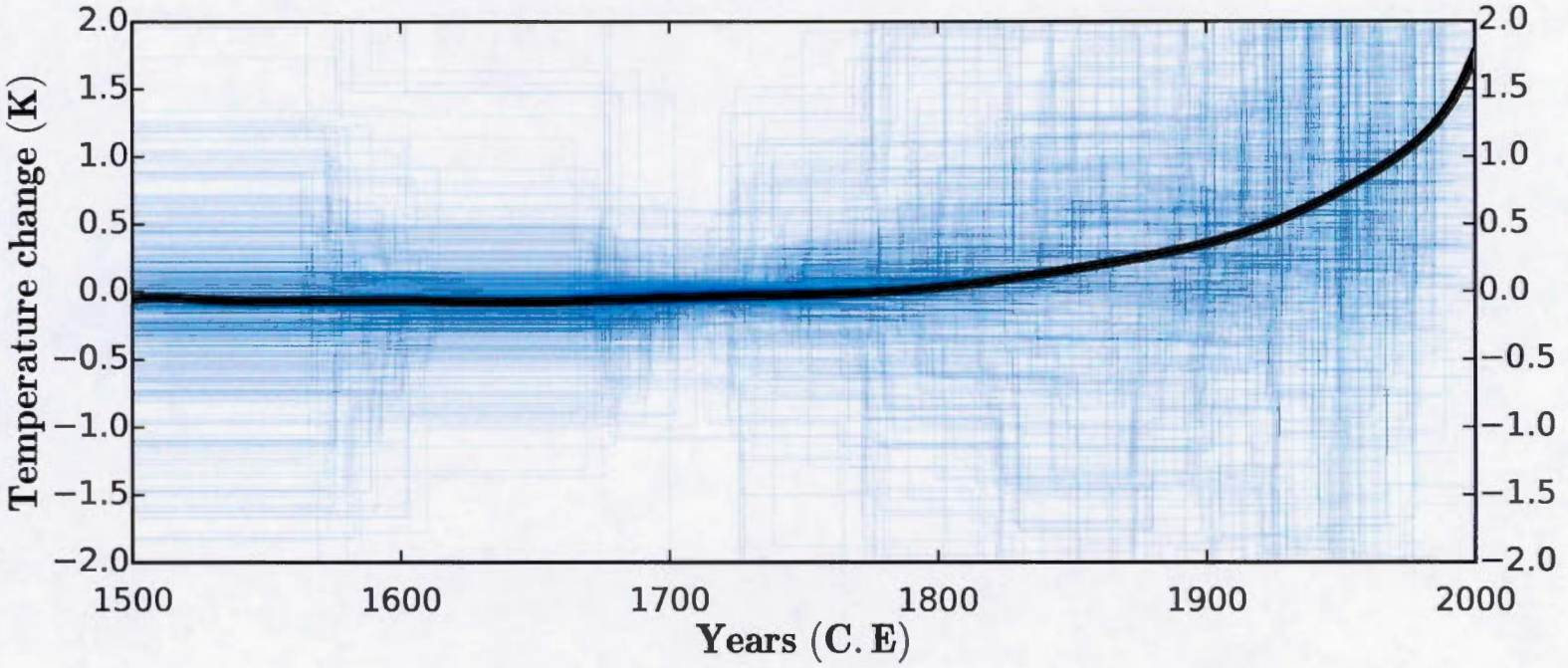

Figure 2.5 Mean North American ground surface temperature change (black). Shown in blue are the 510 ground surface temperature reconstructions inferred from the Monte Carlo inversion.

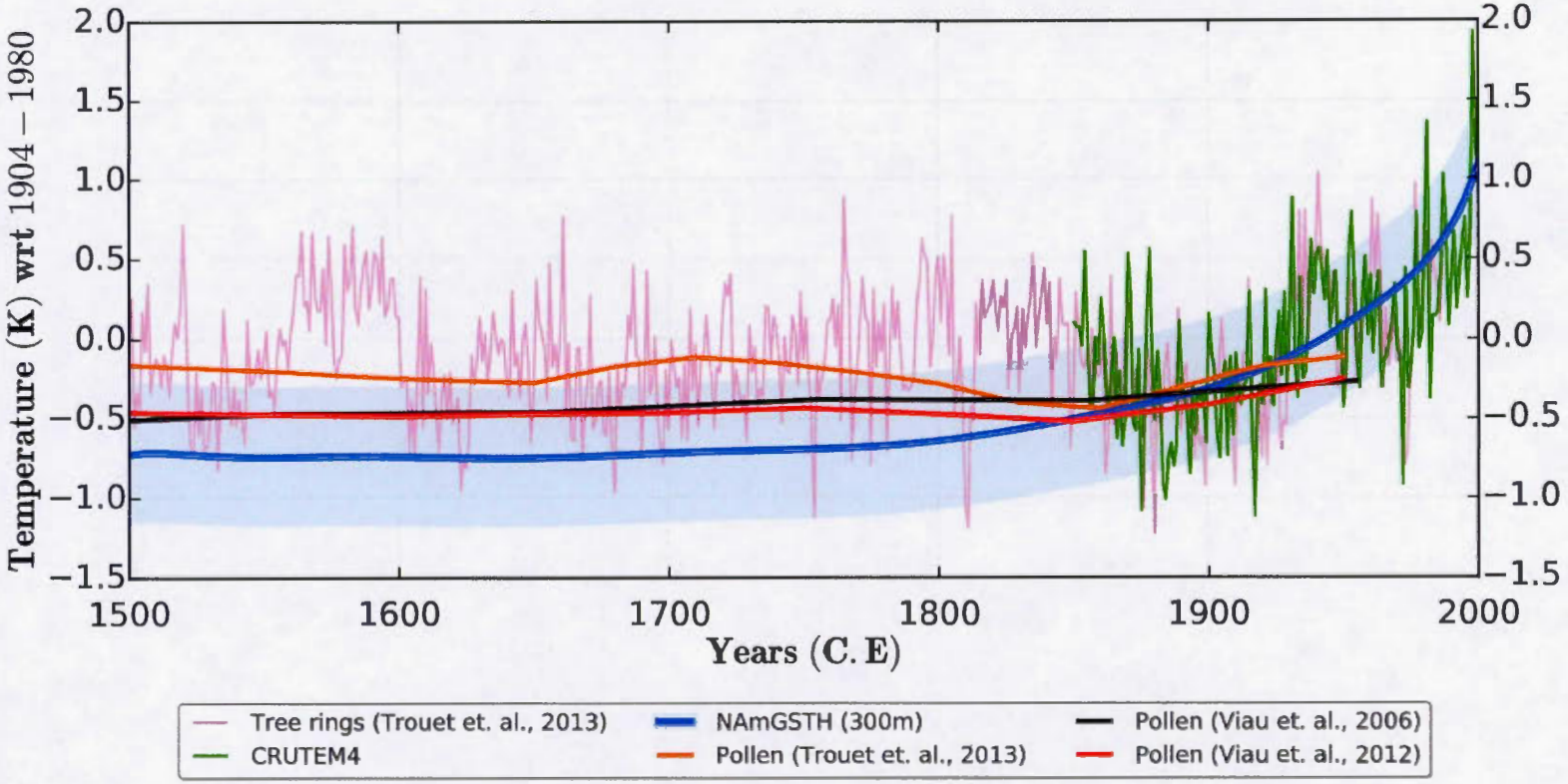

Figure 2.6 Mean North American ground surface temperature history (blue) and maximum temperature range of accepted models (~0.44 K) obtained from the Monte Carlo method (blue shade). Also shown are proxy-based surface air temperature reconstruction for North America from 1500 to 2000 CE. All anomalies are displayed as departures from 1904-1980 mean.

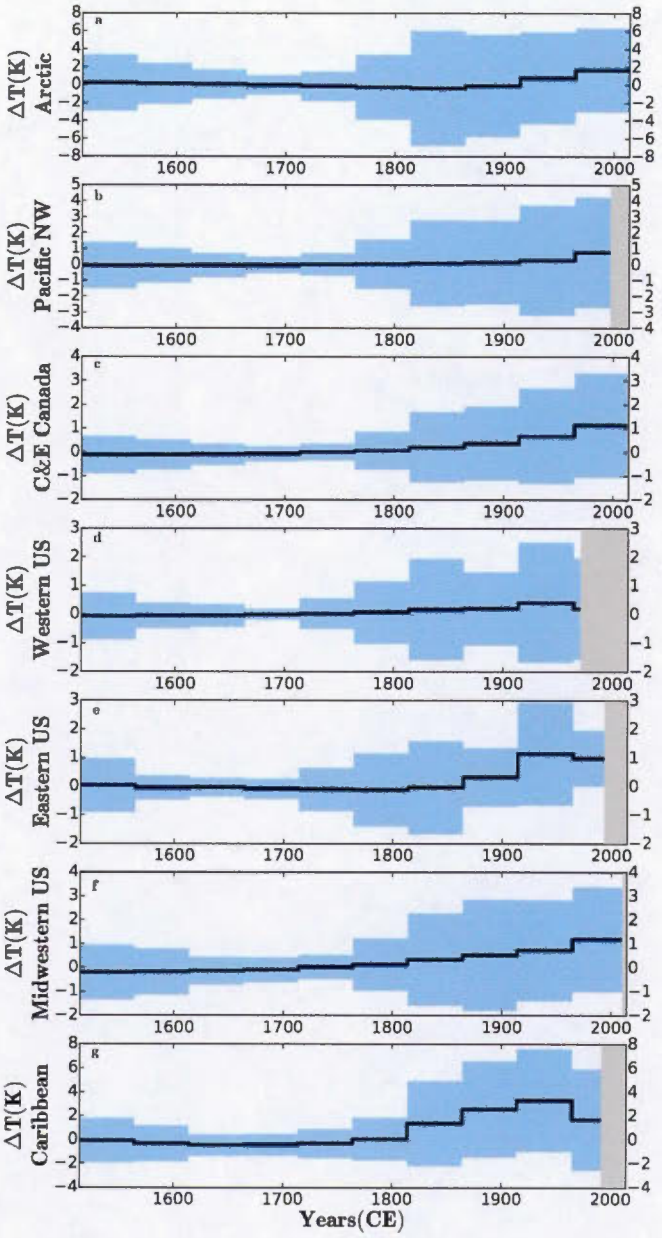

Figure 2.7 Mean ground surface temperature histories (black), the blue shaded areas represent the 95% confidence interval associated with the climate variability of each area. Regional mean temperatures are shown until the year of measurement of the most recent thermal profile in each region. a: Artic (78 sites), b: Pacific Northwest (78 sites), c: Central & Eastern Canada (220 sites), d: Western US (21 sites), e: Eastern US (9 sites), f: Midwestern US (100 sites), g: Caribbean (4 sites).

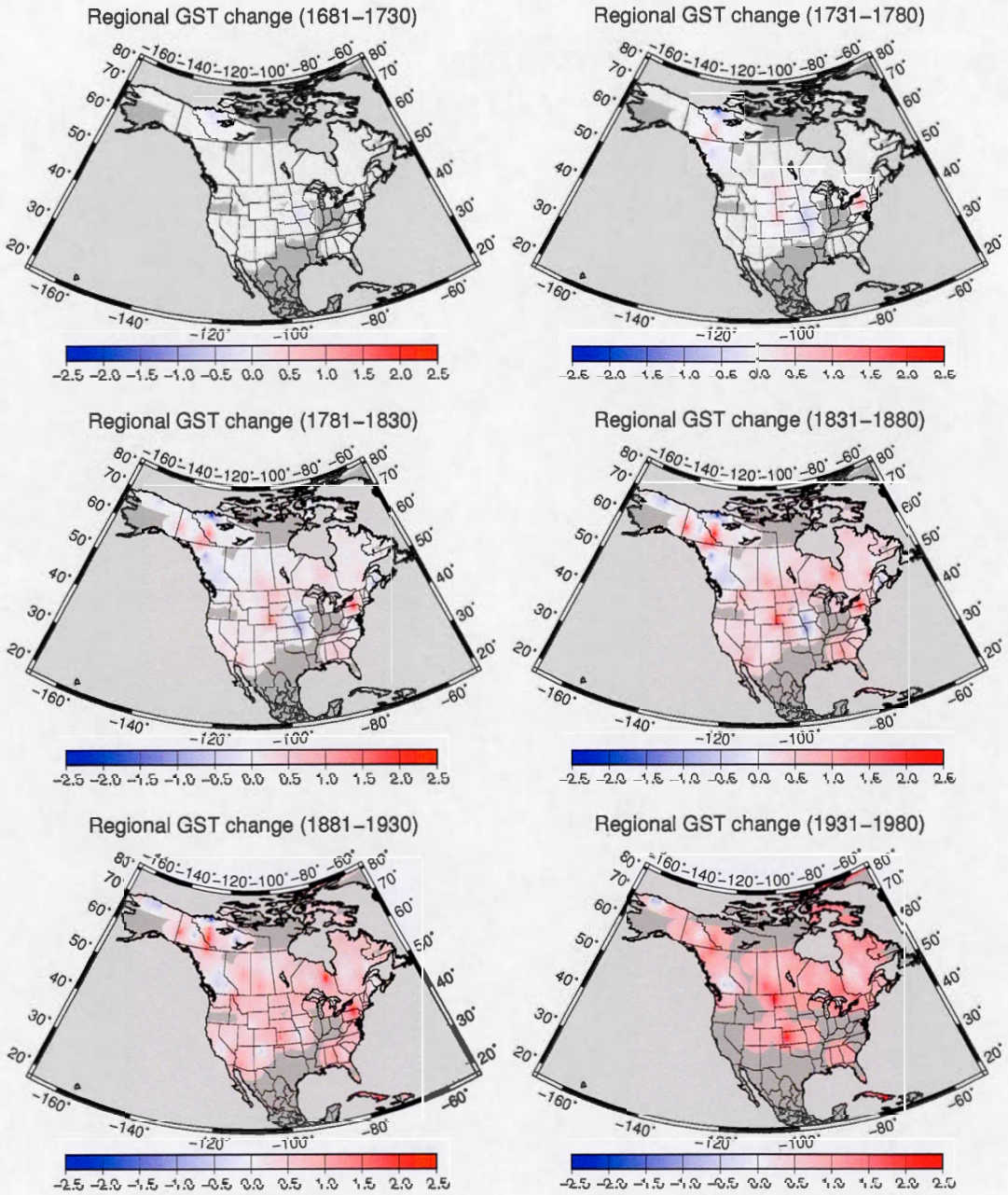

Figure 2.8 Spatial variability of the ground surface temperature variation (in degrees Kelvin) from 1681 to 1980. Each panel shows a regionally interpolated mean ground surface temperature over 50 years. The surface has been masked for zones without at least one datum within a radius of 400 km. Ground surface temperature changes are presented as departures from long-term mean surface temperatures prior to 1500 CE.

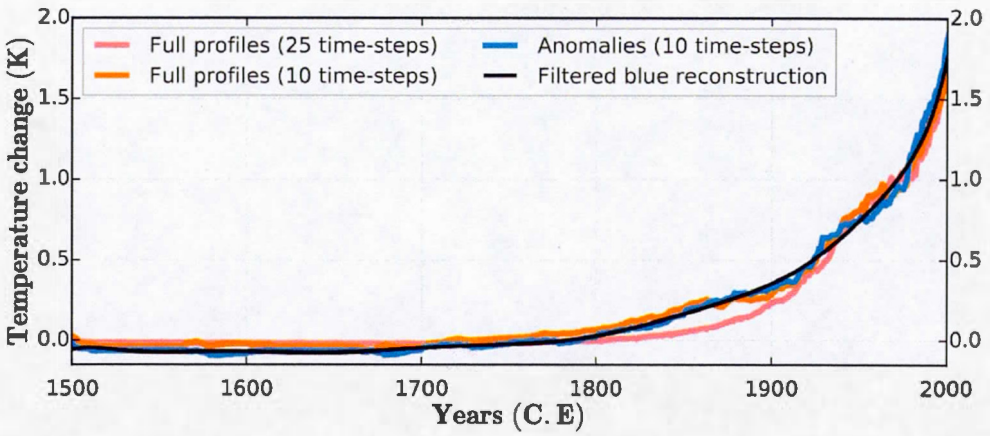

Figure 2.9 Mean North American ground surface temperature histories for different parametrizations. Full inversions have been done for two different time distributions: 10 time-steps using equation (2.15) (orange) and 25 time-steps of 20 years each (red). Furthermore, it has been added a mean ground surface temperature history (blue) obtained from the reconstruction of the anomalies using the linear regression method. Its filtered version (black) was presented in Figure 2.5.

CONCLUSION

The compilation of borehole temperature profiles from previous heat flux studies is worthwhile in terms of expanding regional analysis of GST reconstructions to a continental scale. We presented in Chapter 1 a North American database of thermal profiles measured in boreholes used to reconstruct, in Chapter 2, the GST change for the past 5 centuries. The selection process aimed of checking the quality of these BTPs for climate studies, because that most of them were measured for heat-flux purposes. Moreover, minimum and maximum depths, negligible non-climatic profile perturbations and logging dates are taken into consideration in order to retain and use subsurface geothermal profiles for GST reconstructions.

BTPs allow for the reconstruction of past GST changes. Thus, the inversion of 514 profiles in North America allow to develop maps of GST and and devise past climate trends. The average North American ground surface temperature change reconstructed from boreholes deeper than 300 meters, suggests a warming of $\sim 1.8°C$ between the pre-industrial (1500-1750) and post-industrial (1750-2000) eras. Hoewever, there is a loss of information due to the truncation at 300 meters of all BTPs. For instance, the LIA, a period of cooling that occurred after the medieval warm period, is not observed for the 500-year reconstruction but it is visible for the 1000-year GST reconstruction in the appendix. Furthermore, the multi-decadal temporal resolution of GST histories does not resolve short-term climate perturbations such as volcanic eruptions, but they allow the comparison of long-term climate trends from different regions.

Regional GST means obtained for seven climate-differenced regions, defined within the PAGES NAm2k project (McKay, 2014), suggest a warming range of $\sim 0.5°C$ to $\sim 2.0°C$ with a variability 1σ, no smaller than $0.5°C$. Furthermore, regional GST maps illustrate a warming range of 1°C to 2°C between 1814 and 2014. These warming trends are consistent with multiproxy reconstructions and GCM simulations.

Although the number of borehole temperature profiles for North America has been notably increased in our study, it is still insufficient to guarantee a non spatial-biased regional analysis because their distribution is not sufficiently uniform. It would be interesting to keep sampling boreholes in zones such as Texas, Oklahoma and the south-eastern US, however, it is a slow process that requires time, funding and equipment.

Moreover, reconstructions of past climate trends could be improved using a multi-proxy approach. GST inversions provide robust long-term climate reconstructions for time-scales ranging from hundreds to thousands of years. Such reconstructions would bring out important constraints that past climate GCM outputs must satisfy. This would help for the development of enhanced models, improving reconstructions of past climate histories as well as estimations of future climate projections.

APPENDIX A

A MILLENNIAL RECONSTRUCTION.

GST reconstructions allow for the comparison of regional temperature trends for a given timespan, which is constrained by the maximum depth of the profiles. However, in order to perform these comparisons, it is neccessary to truncate all BTPs at the same depth (Beltrami *et al.*, 2011).

Because there are few deep boreholes, we must truncate at a shallow depth in order to maximize the number of thermal profiles available for a defined region, with thee 300m profiles, the regional analysis is limited to no more than 5 centuries. For instance, in Chapter 2, 510 North American BTPs were truncated at 300 meters which allowed for the reconstruction of the past 500 years.

Moreover, the elimination of deeper parts of profiles results in a loss of information that does not allow observation of long-term variability as for instance the LIA, a cooling period recorded between 1500 C.E and the 1800 C.E. Therefore, we also performed GST reconstructions for the past 1000 years, obtained from 240 North American BTPs truncated at 500 meter.

Figure A.1 presents the millennial North American mean GST history, in 20 timesteps of 50-year length, compared with the previous 500-year reconstruction as well as the surface temperature simulation of GISS-E2-R (Schmidt *et al.*, 2014).

Thus, the LIA is observed in the millennial reconstruction with a temperature change of $\sim -0.4°C$ relative to pre-1500 temperatures. The LIA is not observed in the 500-year reconstruction which illustrates the loss of short-term climate variability due to the maximum depth truncation.

On the other hand, this reconstruction seems to be consistent with the North American surface temperature simulation obtained from GISS-E2-R for the past millennia.

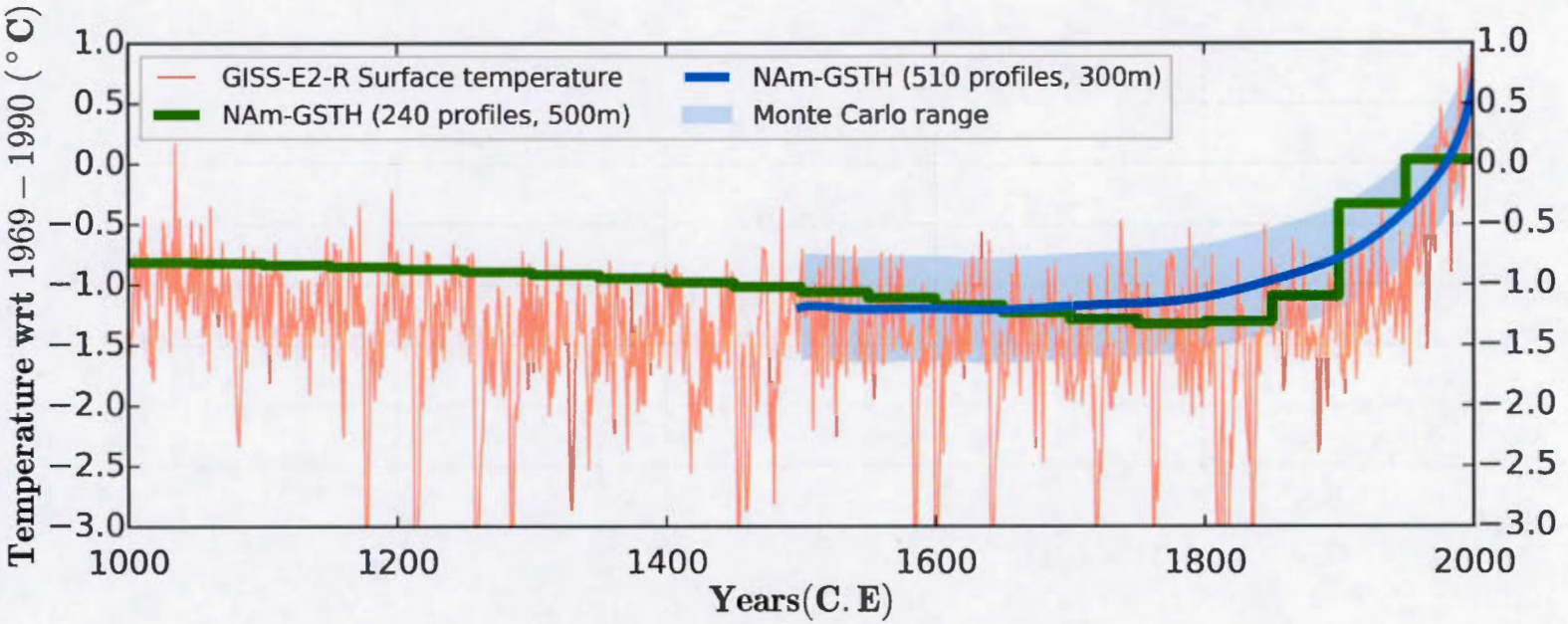

Figure A.1 Millennial North American GST history (green line) compared with North American GST reconstruction for the past 500 years (blue line) presented in Chapter 2. The annual surface temperature simulation from GISS-E2-R (red line) has been added to the figure. All temperatures are relative to the 1969-1990 temperature mean.

APPENDIX B

BOREHOLE TEMPERATURE PROFILE METADATA.

Table B.1 Metadata table attached to the manuscript *North American database for borehole temperature reconstructions.* Latitude and Longitude are in decimal degrees(DD), Max. Depth is in meters(m) and Conductivity is in $\frac{W}{mK}$.

Table B. 1: Supplementary metadata of 510 BTPs suitable for climate reconstructions sorted by latitude (North-South).

Name	Longitude	Latitude	Logging Year	Contact	Country	Max. Depth	Data number	Conductivity
CA-606001_2	-72.897	80.820	1991	Unknown	CA	335.400	55	–
CA-197001_7	-83.080	80.743	1980	Taylor & Judge	CA	749.600	75	3.485
CA-197001_4	-83.080	80.743	1976	Taylor & Judge	CA	736.200	33	3.485
CA-197001_6	-83.080	80.743	1982	Taylor & Judge	CA	734.200	73	3.485
CA-197001_1	-83.080	80.743	1975	Taylor & Judge	CA	731.200	34	3.485
CA-197001_5	-83.080	80.743	1974	Taylor & Judge	CA	735.000	49	3.485
CA-175001_6	-84.070	79.990	1978	Taylor & Judge	CA	875.700	38	2.714
CA-166001_2	-87.020	79.520	1973	Taylor & Judge	CA	441.900	17	2.664
CA-166001_1	-87.020	79.520	1974	Taylor & Judge	CA	441.900	22	2.664
CA-170001_1	-103.253	78.130	1973	Taylor & Judge	CA	549.700	36	3.227
CA-170001_6	-103.253	78.130	1980	Taylor & Judge	CA	561.800	55	3.227
CA-86001_2	-99.760	78.108	1973	Taylor & Judge	CA	655.300	43	3.431
CA-86001_4	-99.760	78.108	1971	Taylor & Judge	CA	705.000	47	3.431
CA-259001_4	-108.492	76.368	1975	Taylor & Judge	CA	399.100	26	–
CA-196001_4	-103.970	76.363	1976	Taylor & Judge	CA	797.500	28	4.386
CA-196001_0	-103.970	76.363	1977	Taylor & Judge	CA	844.600	39	4.386
CA-196001_2	-103.970	76.363	1979	Taylor & Judge	CA	868.700	32	4.386
CA-286001_4	-103.970	76.358	1978	Unknown	CA	890.000	72	3.533
CA-286001_1	-103.970	76.358	1979	Unknown	CA	588.600	37	3.533
CA-286001_3	-103.970	76.358	1980	Unknown	CA	769.600	24	3.533
CA-168001_5	-113.383	74.650	1975	Taylor & Judge	CA	682.000	44	3.683
US-TUL	-155.737	71.189	2014	Gary Clow	US	431.760	3578	–
US-WDS	-155.633	71.159	2014	Gary Clow	US	458.420	2394	–
US-KUY	-156.068	70.931	2002	Gary Clow	US	428.490	3734	–
US-ESN	-154.621	70.917	2002	Gary Clow	US	448.850	3991	–
US-DRP	-153.903	70.879	2003	Gary Clow	US	373.840	3623	–
US-PEA	-159.001	70.716	2003	Gary Clow	US	357.620	3522	–
US-SME	-156.893	70.615	2002	Gary Clow	US	300.530	2432	–
US-KAG	-158.665	70.587	2002	Gary Clow	US	398.580	3374	–
US-ETK	-152.947	70.570	2003	Gary Clow	US	303.720	3007	–
US-ATI	-151.720	70.556	1989	Gary Clow	US	608.280	2886	–
US-NKP	-152.368	70.509	1984	Gary Clow	US	637.030	1979	–
US-IKP	-154.335	70.455	2002	Gary Clow	US	453.310	4076	–
US-FCK	-152.061	70.327	1989	Gary Clow	US	511.150	2429	–

Continued on next page

Table B. 1: Supplementary metadata of 510 BTPs suitable for climate reconstructions sorted by latitude (North-South).

Name	Longitude	Latitude	Logging Year	Contact	Country	Max. Depth	Data number	Conductivity
US-NIN	-152.769	70.257	2002	Gary Clow	US	400.620	3729	–
US-TLK	-161.069	70.206	2003	Gary Clow	US	344.140	3282	–
CA-77001_2	-127.265	69.857	1976	Taylor & Judge	CA	363.300	46	2.464
CA-77001_6	-127.265	69.857	1972	Taylor & Judge	CA	697.000	35	2.464
CA-77001_4	-127.265	69.857	1978	Taylor & Judge	CA	344.400	23	2.464
CA-261001_0	-132.370	69.635	1976	Taylor & Judge	CA	602.900	21	4.443
CA-261001_1	-132.370	69.635	1975	Taylor & Judge	CA	487.400	17	4.443
CA-262001_0	-132.702	69.508	1976	Taylor & Judge	CA	538.000	20	4.009
CA-262001_3	-132.702	69.508	1975	Taylor & Judge	CA	534.290	52	4.009
CA-262001_1	-132.702	69.508	1977	Taylor & Judge	CA	487.700	17	4.009
CA-165001_7	-134.198	69.458	1974	Taylor & Judge	CA	313.900	12	3.361
CA-165001_6	-134.198	69.458	1973	Taylor & Judge	CA	329.200	11	3.361
CA-165001_8	-134.198	69.458	1973	Taylor & Judge	CA	324.500	21	3.361
CA-263001_1	-132.623	69.432	1975	Taylor & Judge	CA	540.910	54	3.426
CA-255001_3	-135.842	69.415	1975	Taylor & Judge	CA	558.100	29	3.318
US-EB1	-148.272	69.400	2013	Gary Clow	US	559.820	3216	–
US-SBE	-152.175	69.380	2002	Gary Clow	US	391.600	3320	–
CA-254001_4	-134.592	69.287	1974	Taylor & Judge	CA	589.800	20	–
CA-176001_9	-134.712	69.213	1974	Taylor & Judge	CA	999.000	50	–
CA-167001_10	-135.342	69.195	1976	Taylor & Judge	CA	593.610	60	3.251
US-AWU	-158.023	69.153	2002	Gary Clow	US	398.630	3630	–
US-LUP	-148.621	69.101	2013	Gary Clow	US	459.910	2805	–
CA-95001_0	-79.063	69.067	1972	Taylor & Judge	CA	435.900	29	2.888
CA-95001_4	-79.063	69.067	1973	Taylor & Judge	CA	441.000	57	2.888
CA-95001_1	-79.063	69.067	1972	Taylor & Judge	CA	455.100	58	2.888
CA-95001_3	-79.063	69.067	1974	Taylor & Judge	CA	438.000	59	2.888
CA-95001_2	-79.063	69.067	1980	Taylor & Judge	CA	437.100	29	2.888
CA-274001_7	-133.563	69.000	1976	Taylor & Judge	CA	1203.000	58	3.312
CA-273001_8	-133.458	68.953	1976	Taylor & Judge	CA	301.400	13	3.23
CA-272001_13	-133.698	68.877	1976	Taylor & Judge	CA	796.790	80	2.781
CA-272001_11	-133.698	68.877	1976	Taylor & Judge	CA	1200.000	60	2.781
CA-76001_1	-131.522	68.533	1972	Taylor & Judge	CA	650.300	43	3.026
CA-76001_0	-131.522	68.533	1971	Taylor & Judge	CA	653.200	44	3.026
CA-76001_2	-131.522	68.533	1970	Taylor & Judge	CA	672.100	43	3.026

Continued on next page

Table B. 1: Supplementary metadata of 510 BTPs suitable for climate reconstructions sorted by latitude (North-South).

Name	Longitude	Latitude	Logging Year	Contact	Country	Max. Depth	Data number	Conductivity
US-LBN	-155.696	68.484	2002	Gary Clow	US	398.500	3147	–
CA-89001_5	-135.550	68.372	1974	Taylor & Judge	CA	790.320	80	3.365
CA-89001_6	-135.550	68.372	1973	Taylor & Judge	CA	498.330	50	3.365
CA-89001_1	-135.550	68.372	1972	Taylor & Judge	CA	1155.500	66	3.365
CA-253001_4	-126.832	67.727	1974	Taylor & Judge	CA	899.900	90	–
CA-253001_3	-126.832	67.727	1976	Taylor & Judge	CA	827.900	52	–
CA-151001_2	-124.595	65.557	1972	Taylor & Judge	CA	354.800	24	1.94
CA-88005_0	-126.880	65.285	1966	Taylor & Judge	CA	396.200	12	–
CA-88004_0	-126.867	65.285	1966	Taylor & Judge	CA	396.200	14	–
CA-400004_0	-135.153	62.787	1992	Unknown	CA	459.700	44	4.885
CA-400006_0	-135.152	62.785	1992	Unknown	CA	470.000	46	4.802
CA-400009_0	-135.155	62.783	1992	Unknown	CA	341.200	34	4.397
CA-703004_0	-138.832	62.738	1993	Lewis et al	CA	418.500	31	3.591
CA-066-0	-114.420	62.510	1975	A.M. Jessop	CA	422.300	53	2.5
CA-290-1	-129.220	62.470	1981	A.M. Jessop	CA	387.000	15	2.5
CA-0614	-73.575	61.692	2006	J-C Mareschal	CA	504.990	53	2.933
CA-0615	-73.589	61.689	2006	J-C Mareschal	CA	403.596	42	2.712
CA-707005_0	-130.593	61.465	1997	Lewis et al	CA	349.600	69	3.788
CA-289-1	-133.750	60.990	1981	A.M. Jessop	CA	451.900	28	2.5
CA-289-2	-133.750	60.990	1981	A.M. Jessop	CA	309.100	16	2.5
CA-289-4	-133.750	60.990	1981	A.M. Jessop	CA	571.300	72	2.5
CA-122003_0	-135.183	60.750	1977	Unknown	CA	387.700	25	2.919
CA-122001_0	-135.053	60.623	1976	Jessop et al	CA	485.200	31	–
CA-705004_0	-128.945	60.557	1993	Lewis et al	CA	424.400	43	–
CA-705003_0	-128.945	60.557	1993	Lewis et al	CA	436.600	43	–
CA-139006_0	-131.603	60.010	1983	Unknown	CA	300.500	18	–
CA-431001_0	-130.328	59.923	1985	Lewis et al	CA	424.900	39	3.388
CA-188002_0	-133.402	59.713	1973	Jessop et al	CA	304.800	20	–
CA-188001_0	-133.413	59.712	1973	Jessop et al	CA	350.500	23	–
CA-398002_0	-133.590	58.742	1991	Unknown	CA	640.100	63	3.054
CA-9920	-109.541	58.377	1999	J-C Mareschal	CA	330.000	33	3.5
CA-9923	-109.520	58.230	1999	J-C Mareschal	CA	400.000	37	6
CA-9922	-109.518	58.229	1999	J-C Mareschal	CA	730.000	69	6
CA-010-0	-130.850	57.890	1978	A.M. Jessop	CA	422.100	54	2.1

Continued on next page

Table B. 1: Supplementary metadata of 510 BTPs suitable for climate reconstructions sorted by latitude (North-South).

Name	Longitude	Latitude	Logging Year	Contact	Country	Max. Depth	Data number	Conductivity
CA-9520	-100.438	56.909	1995	J-C Mareschal	CA	579.556	59	3.8
CA-9516	-100.435	56.909	1995	J-C Mareschal	CA	589.215	61	3.6
CA-9517	-100.441	56.909	1995	J-C Mareschal	CA	557.544	55	3.5
CA-149-2	-100.950	56.900	1985	A.M. Jessop	CA	493.800	71	3.1
CA-0019	-101.082	56.891	2000	J-C Mareschal	CA	671.526	76	3.264
CA-0018	-101.071	56.889	2000	J-C Mareschal	CA	385.457	46	3.463
CA-9614	-101.102	56.827	1996	J-C Mareschal	CA	419.419	46	3.8
CA-149-1	-101.100	56.800	1985	K. Wang	CA	588.900	74	2.53
CA-9514	-100.950	56.734	1995	J-C Mareschal	CA	375.877	39	2.5
CA-390008_0	-130.428	56.653	1990	Unknown	CA	390.200	77	2.607
CA-9519	-101.634	56.631	1995	J-C Mareschal	CA	422.861	44	3
CA-150-1	-101.650	56.630	1985	K. Wang	CA	382.700	57	3.53
CA-115-3	-126.690	56.600	1975	A.M. Jessop	CA	320.000	20	2.5
CA-9822	-62.108	56.330	1998	J-C Mareschal	CA	641.137	70	1.9
CA-9821	-62.108	56.328	1998	J-C Mareschal	CA	813.632	95	2.4
CA-9823	-62.055	56.319	1998	J-C Mareschal	CA	899.480	89	2.2
CA-9824	-62.055	56.319	1998	J-C Mareschal	CA	946.917	95	1.9
CA-9918	-103.116	56.159	1999	J-C Mareschal	CA	393.923	40	2.4
CA-9603	-103.707	56.130	1996	J-C Mareschal	CA	569.896	59	3.5
CA-9604	-103.707	56.130	1996	J-C Mareschal	CA	540.919	55	2.9
CA-9605	-103.700	56.130	1996	J-C Mareschal	CA	463.640	47	3.1
CA-375010_0	-130.047	56.075	1991	Unknown	CA	572.300	58	3.82
CA-0016	-97.619	55.926	2000	J-C Mareschal	CA	860.100	97	4.077
CA-9409	-97.678	55.898	1994	J-C Mareschal	CA	469.775	52	3.7
CA-9808	-102.740	55.869	1998	J-C Mareschal	CA	419.566	42	2.2
CA-9813	-97.777	55.828	1998	J-C Mareschal	CA	672.286	85	3.4
CA-9812	-97.761	55.828	1998	J-C Mareschal	CA	897.582	96	3.2
CA-9413	-97.813	55.746	1994	J-C Mareschal	CA	555.122	52	3
CA-9407	-97.823	55.740	1994	J-C Mareschal	CA	991.259	100	5
CA-138-0	-97.770	55.730	1985	K. Wang	CA	595.100	75	3.38
CA-9405	-97.897	55.700	1994	J-C Mareschal	CA	521.347	55	3.5
CA-0017	-97.860	55.671	2000	J-C Mareschal	CA	916.244	95	3.809
CA-0115	-98.270	55.540	2001	J-C Mareschal	CA	334.920	34	3.44
CA-0114	-98.230	55.510	2001	J-C Mareschal	CA	586.120	67	3.44

Continued on next page

Table B. 1: Supplementary metadata of 510 BTPs suitable for climate reconstructions sorted by latitude (North-South).

Name	Longitude	Latitude	Logging Year	Contact	Country	Max. Depth	Data number	Conductivity
CA-0022	-98.131	55.492	2000	J-C Mareschal	CA	374.524	41	3.828
CA-9410	-98.131	55.488	1994	J-C Mareschal	CA	386.471	38	2.9
CA-0020	-98.136	55.488	2000	J-C Mareschal	CA	325.661	35	3.774
CA-0015	-98.131	55.488	2000	J-C Mareschal	CA	376.916	38	3.828
CA-9814	-98.126	55.486	1998	J-C Mareschal	CA	345.482	35	4.8
CA-9815	-98.126	55.486	1998	J-C Mareschal	CA	347.580	35	4.8
CA-9411	-98.132	55.486	1994	J-C Mareschal	CA	840.346	86	3.4
CA-9816	-98.126	55.486	1998	J-C Mareschal	CA	380.000	38	4.8
CA-0021	-98.132	55.486	2000	J-C Mareschal	CA	343.320	34	3.884
CA-389001_0	-129.828	55.445	1989	Unknown	CA	490.300	48	3.393
CA-389004_0	-129.828	55.440	1989	Unknown	CA	457.000	43	2.925
CA-9601	-105.020	55.292	1996	J-C Mareschal	CA	880.000	87	2.8
CA-9905	-101.357	55.198	1999	J-C Mareschal	CA	300.000	30	3.1
CA-9702	-98.458	55.171	1997	J-C Mareschal	CA	679.565	70	2.8
CA-9617	-100.759	55.164	1996	J-C Mareschal	CA	307.757	31	–
CA-9804	-100.759	55.164	1998	J-C Mareschal	CA	307.764	32	3.6
CA-9907	-100.563	54.932	1999	J-C Mareschal	CA	523.335	60	3.4
CA-137-1	-99.970	54.890	1985	K. Wang	CA	353.200	125	3.73
CA-9301	-98.644	54.875	1993	J-C Mareschal	CA	809.967	102	2.8
CA-9302	-98.644	54.875	1993	J-C Mareschal	CA	543.407	78	3.1
CA-9308	-99.981	54.868	1993	J-C Mareschal	CA	645.341	90	3.1
CA-9505	-101.740	54.858	1995	J-C Mareschal	CA	568.340	60	3.1
CA-9309	-99.954	54.854	1993	J-C Mareschal	CA	686.083	79	3.8
CA-9801	-100.110	54.846	1998	J-C Mareschal	CA	714.997	81	3.1
CA-9807	-101.570	54.790	1998	J-C Mareschal	CA	446.922	62	5.7
CA-9806	-101.570	54.790	1998	J-C Mareschal	CA	498.781	65	5.2
CA-0712	-71.283	54.789	2007	J-C Mareschal	CA	561.190	68	–
CA-0713	-71.837	54.788	2007	J-C Mareschal	CA	460.335	57	–
CA-9307	-101.888	54.787	1993	J-C Mareschal	CA	577.388	72	3.6
CA-0714	-71.294	54.784	2007	J-C Mareschal	CA	383.790	45	–
CA-9906	-101.838	54.773	1999	J-C Mareschal	CA	1418.467	175	3.6
CA-9818	-100.206	54.759	1998	J-C Mareschal	CA	667.826	91	3.6
CA-9305	-101.832	54.720	1993	J-C Mareschal	CA	870.000	104	3.6
CA-9610	-102.058	54.658	1996	J-C Mareschal	CA	534.407	70	3.6

Continued on next page

Table B. 1: Supplementary metadata of 510 BTPs suitable for climate reconstructions sorted by latitude (North-South).

Name	Longitude	Latitude	Logging Year	Contact	Country	Max. Depth	Data number	Conductivity
CA-9609	-102.059	54.658	1996	J-C Mareschal	CA	585.161	75	3
CA-136-1	-102.040	54.640	1985	K. Wang	CA	465.000	171	2.82
CA-9608	-102.829	54.636	1996	J-C Mareschal	CA	560.237	58	3.9
CA-9506	-103.200	54.575	1995	J-C Mareschal	CA	616.289	68	3.6
CA-9306	-100.381	54.571	1993	J-C Mareschal	CA	432.620	64	2.7
CA-9501	-100.230	54.214	1995	J-C Mareschal	CA	1180.000	112	3.5
CA-9502	-100.230	54.214	1995	J-C Mareschal	CA	352.378	38	3.9
CA-382001_0	-130.588	54.023	1988	Unknown	CA	428.200	38	3.145
CA-0405	-76.554	53.529	2004	J-C Mareschal	CA	559.850	71	2.89
CA-0715	-75.215	53.466	2007	J-C Mareschal	CA	437.037	55	–
CA-357004_0	-130.162	53.367	1984	Unknown	CA	1360.000	65	3.063
CA-357017_0	-130.167	53.367	1984	Unknown	CA	722.000	36	–
CA-0716	-73.929	53.318	2007	J-C Mareschal	CA	478.518	57	–
CA-658001_0	-113.883	53.167	1968	Majorowicz & Jessop	CA	2865.100	183	3.3
CA-1014	-86.300	52.742	2010	J-C Mareschal	CA	762.050	79	3.082
CA-1012	-86.295	52.740	2010	J-C Mareschal	CA	760.498	84	3.184
CA-1015	-86.303	52.740	2010	J-C Mareschal	CA	806.480	79	3.119
CA-1013	-86.295	52.740	2010	J-C Mareschal	CA	404.621	46	3.088
CA-0502	-76.074	52.700	2005	J-C Mareschal	CA	542.569	67	2.47
CA-081-1	-121.560	52.630	1985	A.M. Jessop	CA	311.200	20	2.55
CA-475001_0	-119.273	52.392	1983	Unknown	CA	321.000	28	–
CA-0506	-75.804	52.205	2005	J-C Mareschal	CA	742.970	79	2.63
CA-JM-a	-107.120	52.020	1996	J. Majorowicz	CA	529.800	104	1.6
CA-015-0	-89.600	51.830	1978	K. Wang	CA	500.400	87	2.69
CA-015-1	-89.600	51.830	1978	K. Wang	CA	605.600	75	2.69
CA-0605	-90.353	51.507	2006	J-C Mareschal	CA	802.330	85	2.989
CA-0608	-90.352	51.504	2006	J-C Mareschal	CA	736.350	86	2.597
CA-369001_0	-123.623	51.465	1992	Unknown	CA	814.100	82	4.018
CA-369002_0	-123.622	51.465	1990	Unknown	CA	438.400	44	3.931
CA-372003_0	-120.065	51.382	1987	Bentkowski & Lewis	CA	317.700	32	3.036
CA-372002_0	-120.065	51.380	1987	Bentkowski & Lewis	CA	411.200	41	2.943
CA-355002_0	-119.803	51.145	1985	Unknown	CA	737.310	100	3.458
CA-0203	-93.760	51.104	2002	J-C Mareschal	CA	575.168	74	3.36
CA-0201	-93.734	51.050	2002	J-C Mareschal	CA	2028.609	201	3.59

Continued on next page

Table B. 1: Supplementary metadata of 510 BTPs suitable for climate reconstructions sorted by latitude (North-South).

Name	Longitude	Latitude	Logging Year	Contact	Country	Max. Depth	Data number	Conductivity
CA-0002	-93.716	51.033	2000	J-C Mareschal	CA	1724.232	177	3.18
CA-9511	-74.467	51.014	1995	J-C Mareschal	CA	513.175	51	3
CA-9512	-74.468	51.014	1995	J-C Mareschal	CA	558.565	56	2.9
CA-0001	-93.814	51.013	2000	J-C Mareschal	CA	804.784	97	3.19
CA-083-0	-94.200	51.000	1978	A.M. Jessop	CA	311.200	35	4.09
CA-0003	-93.107	50.891	2000	J-C Mareschal	CA	337.683	40	5
CA-0004	-93.104	50.879	2000	J-C Mareschal	CA	496.198	62	4.53
CA-0005	-92.824	50.830	2000	J-C Mareschal	CA	924.568	98	4.87
CA-339001_25	-123.670	50.722	1983	Lewis et al	CA	457.200	91	3.473
CA-339001_26	-123.670	50.722	1983	Lewis et al	CA	450.200	45	3.473
CA-016-0	-90.480	50.710	1978	K. Wang	CA	600.700	105	3
CA-016-1	-90.480	50.710	1978	K. Wang	CA	596.800	74	3
CA-353010_0	-127.505	50.618	1990	Unknown	CA	389.800	39	2.761
CA-161001_0	-120.970	50.477	1985	Lewis et al	CA	461.800	15	2.954
CA-298-1	-95.440	50.430	1982	A.M. Jessop	CA	419.700	131	3.18
CA-298-2	-95.420	50.420	1986	A.M. Jessop	CA	303.300	81	3.18
CA-298-4	-95.450	50.420	1982	A.M. Jessop	CA	301.800	92	3.18
CA-298-3	-95.410	50.420	1986	A.M. Jessop	CA	308.500	95	3.18
CA-464001_0	-123.023	50.388	1982	Unknown	CA	317.000	29	–
CA-0308	-87.953	50.383	2003	J-C Mareschal	CA	422.560	45	2.75
CA-0306	-87.949	50.382	2003	J-C Mareschal	CA	351.809	38	2.83
CA-0307	-87.950	50.381	2003	J-C Mareschal	CA	369.590	40	3.05
CA-9402	-66.446	50.295	1994	J-C Mareschal	CA	460.000	45	2
CA-0111	-94.566	50.264	2001	J-C Mareschal	CA	303.767	32	3.1
CA-145-15	-95.850	50.250	1983	A.M. Jessop	CA	389.400	119	2.62
CA-9820	-66.639	50.213	1998	J-C Mareschal	CA	1820.000	179	2.5
CA-9400	-66.640	50.210	1994	J-C Mareschal	CA	1010.000	98	2.1
CA-456001_0	-123.537	50.203	1982	Lewis et al	CA	320.000	32	2.15
CA-0705	-87.608	50.162	2007	J-C Mareschal	CA	483.028	51	4.761
CA-344001_1	-123.258	50.110	1982	Lewis et al	CA	463.300	153	3.207
CA-126-0	-85.900	50.100	1986	K. Wang	CA	596.200	75	3.38
CA-0310	-89.089	50.063	2003	J-C Mareschal	CA	390.000	39	2.22
CA-343001_13	-123.197	50.025	1981	Lewis et al	CA	413.900	18	2.58
CA-343001_12	-123.197	50.025	1981	Lewis et al	CA	397.200	23	2.58

Continued on next page

Table B. 1: Supplementary metadata of 510 BTPs suitable for climate reconstructions sorted by latitude (North-South).

Name	Longitude	Latitude	Logging Year	Contact	Country	Max. Depth	Data number	Conductivity
CA-343001_11	-123.197	50.025	1981	Lewis et al	CA	362.400	16	2.58
CA-343001_14	-123.197	50.025	1981	Lewis et al	CA	438.300	22	2.58
CA-1010	-87.652	50.019	2010	J-C Mareschal	CA	397.730	48	–
CA-310001_19	-119.787	49.958	1980	Davis & Lewis	CA	334.400	20	2.771
CA-310001_22	-119.787	49.958	1980	Davis & Lewis	CA	334.700	44	2.771
CA-152-2	-56.050	49.910	1978	A.M. Jessop	CA	430.100	28	3.4
CA-152-1	-56.050	49.910	1978	K. Wang	CA	472.400	30	3.83
CA-152-3	-56.080	49.900	1975	A.M. Jessop	CA	324.000	22	3.56
CA-9009	-74.170	49.899	1990	J-C Mareschal	CA	571.033	75	3.2
CA-0007	-90.897	49.894	2000	J-C Mareschal	CA	895.631	96	3.84
CA-9008	-74.174	49.891	1990	J-C Mareschal	CA	593.236	75	3.4
CA-9012	-74.333	49.881	1990	J-C Mareschal	CA	317.501	59	3.2
CA-9010	-74.333	49.881	1990	J-C Mareschal	CA	440.157	64	3.3
CA-117-2	-90.880	49.880	1975	A.M. Jessop	CA	437.800	26	2.5
CA-069-0	-74.350	49.880	1978	A.M. Jessop	CA	597.500	21	3.4
CA-0006	-90.996	49.877	2000	J-C Mareschal	CA	653.050	86	4.77
CA-0703	-87.739	49.829	2007	J-C Mareschal	CA	429.411	42	3.278
CA-1001	-87.673	49.815	2010	J-C Mareschal	CA	475.086	62	3.346
CA-1002	-87.674	49.814	2010	J-C Mareschal	CA	505.583	65	3.381
CA-8743	-74.809	49.797	1987	J-C Mareschal	CA	503.938	59	3.2
CA-9510	-74.031	49.790	1995	J-C Mareschal	CA	784.960	93	4
CA-8742	-74.809	49.787	1987	J-C Mareschal	CA	518.842	57	3.5
CA-438-2	-77.640	49.780	1987	K. Wang	CA	375.500	110	3.52
CA-017-0	-91.370	49.770	1978	K. Wang	CA	597.400	74	3.02
CA-0701	-93.135	49.760	2007	J-C Mareschal	CA	853.094	93	3.13
CA-074-0	-116.860	49.760	1974	A.M. Jessop	CA	443.400	32	2.5
CA-0108	-92.610	49.758	2001	J-C Mareschal	CA	770.713	81	3.11
CA-386015_0	-124.547	49.757	1989	Lewis et al	CA	393.400	36	3.307
CA-0107	-92.615	49.757	2001	J-C Mareschal	CA	733.859	74	3.71
CA-0309	-89.188	49.752	2003	J-C Mareschal	CA	810.000	81	2.49
CA-8744	-77.734	49.716	1987	J-C Mareschal	CA	600.000	60	3.3
CA-8746	-77.739	49.716	1987	J-C Mareschal	CA	600.000	59	3.3
CA-8745	-77.734	49.713	1987	J-C Mareschal	CA	600.000	59	3.6
CA-438-1	-77.740	49.710	1987	K. Wang	CA	599.800	172	3.52

Continued on next page

Table B. 1: Supplementary metadata of 510 BTPs suitable for climate reconstructions sorted by latitude (North-South).

Name	Longitude	Latitude	Logging Year	Contact	Country	Max. Depth	Data number	Conductivity
CA-104002_0	-116.000	49.700	1968	Lewis et al	CA	313.700	22	3.405
CA-104001_0	-116.000	49.700	1968	Lewis et al	CA	380.400	24	4.539
CA-104008_0	-116.000	49.700	1971	Unknown	CA	518.160	32	3.459
CA-104005_0	-116.000	49.700	1971	Unknown	CA	911.350	60	3.286
CA-104003_0	-116.000	49.700	1969	Unknown	CA	579.100	38	–
CA-104011_0	-116.000	49.700	1976	Lewis et al	CA	354.500	24	3.225
CA-104014_0	-116.000	49.700	1976	Lewis et al	CA	533.400	34	3.991
CA-104-2	-115.890	49.690	1975	A.M. Jessop	CA	313.700	21	2.5
CA-013-0	-83.530	49.690	1978	K. Wang	CA	575.900	114	3.14
CA-013-1	-83.540	49.690	1978	K. Wang	CA	571.800	72	3.14
CA-104-3	-115.940	49.680	1975	A.M. Jessop	CA	579.100	34	2.5
CA-8740	-75.870	49.620	1987	J-C Mareschal	CA	306.045	41	3.8
CA-107001_0	-123.160	49.612	1973	Lewis et al	CA	304.800	18	4.778
CA-8736	-75.876	49.611	1987	J-C Mareschal	CA	334.835	30	3.1
CA-495001_0	-119.688	49.608	1990	Unknown	CA	706.100	130	–
CA-9204	-75.980	49.603	1992	J-C Mareschal	CA	510.955	78	3.2
CA-0013	-85.810	49.583	2000	J-C Mareschal	CA	1434.731	145	3.31
CA-163-1	-125.610	49.580	1985	A.M. Jessop	CA	596.200	38	3.35
CA-310002_20	-119.652	49.570	1980	Davis & Lewis	CA	450.200	21	2.551
CA-310002_14	-119.652	49.570	1980	Davis & Lewis	CA	352.600	27	2.551
CA-310002_18	-119.652	49.570	1980	Davis & Lewis	CA	428.600	23	2.551
CA-310002_17	-119.652	49.570	1980	Davis & Lewis	CA	410.600	23	2.551
CA-310002_16	-119.652	49.570	1980	Davis & Lewis	CA	392.300	24	2.551
CA-310002_15	-119.652	49.570	1980	Davis & Lewis	CA	374.000	20	2.551
CA-310002_19	-119.652	49.570	1980	Davis & Lewis	CA	442.000	23	2.551
CA-9207	-76.173	49.494	1992	J-C Mareschal	CA	610.000	76	3
CA-9206	-76.173	49.493	1992	J-C Mareschal	CA	450.000	60	3.1
CA-9211	-74.618	49.484	1992	J-C Mareschal	CA	480.000	67	2.9
CA-9209	-74.611	49.479	1992	J-C Mareschal	CA	485.782	64	2.9
CA-012-0	-82.380	49.420	1978	K. Wang	CA	594.700	78	2.64
CA-159013_1	-121.977	49.337	1992	Unknown	CA	318.600	30	3.716
CA-159013_0	-121.977	49.337	1992	Unknown	CA	318.500	31	3.716
CA-0711	-88.801	49.336	2007	J-C Mareschal	CA	566.187	58	2.14
CA-0104	-93.720	49.293	2001	J-C Mareschal	CA	637.944	74	3.53

Continued on next page

Table B. 1: Supplementary metadata of 510 BTPs suitable for climate reconstructions sorted by latitude (North-South).

Name	Longitude	Latitude	Logging Year	Contact	Country	Max. Depth	Data number	Conductivity
CA-9203	-76.653	49.244	1992	J-C Mareschal	CA	880.000	107	4.2
CA-9202	-76.654	49.242	1992	J-C Mareschal	CA	880.000	106	4.3
CA-084-2	-85.810	49.190	1978	A.M. Jessop	CA	583.600	19	3.04
CA-084-3	-85.850	49.190	1978	K. Wang	CA	599.800	39	3.28
CA-0311	-88.873	49.185	2003	J-C Mareschal	CA	348.560	35	2.16
CA-084-7	-85.850	49.180	1978	K. Wang	CA	598.900	39	3.15
CA-084-1	-85.850	49.180	1978	K. Wang	CA	587.000	38	3.33
CA-084-6	-85.850	49.180	1978	K. Wang	CA	601.100	39	3.46
CA-084-4	-85.810	49.180	1978	K. Wang	CA	598.900	39	3.27
CA-0009	-89.605	49.172	2000	J-C Mareschal	CA	780.995	96	2.69
CA-0008	-89.605	49.171	2000	J-C Mareschal	CA	675.541	86	2.82
CA-0611	-85.772	49.169	2006	J-C Mareschal	CA	1799.222	180	3
CA-0012	-85.825	49.167	2000	J-C Mareschal	CA	956.202	96	2.95
CA-0610	-85.397	49.153	2006	J-C Mareschal	CA	1746.730	183	2.873
CA-072-2	-117.190	49.150	1974	A.M. Jessop	CA	590.200	34	2.5
CA-0302	-91.360	49.140	2003	J-C Mareschal	CA	412.080	43	3.76
CA-011-0	-80.940	49.100	1978	A.M. Jessop	CA	454.800	55	2.51
CA-358004_0	-123.852	49.080	1988	Lewis et al	CA	369.110	100	–
CA-0112	-85.957	49.028	2001	J-C Mareschal	CA	800.000	79	3.37
CA-370010_0	-123.000	49.000	1994	Unknown	CA	302.400	61	–
CA-370010_1	-123.000	49.000	1994	Unknown	CA	302.400	85	–
CA-103-6	-65.530	48.950	1975	A.M. Jessop	CA	535.200	34	3.88
CA-103-3	-65.530	48.950	1975	A.M. Jessop	CA	432.600	30	3.88
CA-103-5	-65.530	48.950	1975	A.M. Jessop	CA	368.900	23	3.88
CA-0312	-87.920	48.920	2003	J-C Mareschal	CA	422.738	46	3.28
CA-014-0	-86.980	48.860	1978	K. Wang	CA	596.500	74	2.91
CA-096-0	-64.680	48.860	1986	K. Wang	CA	594.400	38	3.36
CA-0102	-94.013	48.832	2001	J-C Mareschal	CA	723.497	74	3.68
CA-8720	-66.013	48.831	1987	J-C Mareschal	CA	600.000	60	3.3
CA-0106	-94.015	48.829	2001	J-C Mareschal	CA	460.097	47	3.99
CA-8721	-66.021	48.821	1987	J-C Mareschal	CA	500.000	50	3
CA-0708	-86.315	48.800	2007	J-C Mareschal	CA	355.700	38	2.244
CA-0707	-86.317	48.797	2007	J-C Mareschal	CA	389.691	42	2.321
CA-8723	-66.130	48.797	1987	J-C Mareschal	CA	520.003	57	2.7

Continued on next page

Table B. 1: Supplementary metadata of 510 BTPs suitable for climate reconstructions sorted by latitude (North-South).

Name	Longitude	Latitude	Logging Year	Contact	Country	Max. Depth	Data number	Conductivity
CA-8725	-66.149	48.790	1987	J-C Mareschal	CA	349.826	35	3.1
CA-0314	-81.390	48.702	2003	J-C Mareschal	CA	986.768	105	2.32
CA-0315	-81.390	48.702	2003	J-C Mareschal	CA	1372.700	159	2.32
CA-1009	-93.068	48.701	2010	J-C Mareschal	CA	766.395	78	2.375
CA-156-0	-78.440	48.650	1978	K. Wang	CA	356.300	23	3.66
CA-321001_3	-123.448	48.650	1990	Lewis et al	CA	302.000	47	2.672
CA-321001_1	-123.448	48.650	1990	Lewis et al	CA	304.000	22	2.672
CA-0209	-92.095	48.621	2002	J-C Mareschal	CA	369.912	36	3.13
CA-0304	-90.768	48.543	2003	J-C Mareschal	CA	586.592	61	3.94
CA-0303	-90.769	48.540	2003	J-C Mareschal	CA	596.919	61	3.94
CA-9214	-77.691	48.531	1992	J-C Mareschal	CA	620.000	60	3.6
CA-9212	-77.693	48.531	1992	J-C Mareschal	CA	370.000	54	3.6
CA-006-0	-72.250	48.530	1978	K. Wang	CA	595.300	39	2.5
CA-9213	-77.686	48.529	1992	J-C Mareschal	CA	640.000	80	3.6
CA-9114	-79.719	48.520	1991	J-C Mareschal	CA	419.992	49	3.6
CA-9116	-79.721	48.520	1991	J-C Mareschal	CA	373.676	48	3.3
CA-436-3	-82.430	48.300	1986	A.M. Jessop	CA	376.700	113	3.12
CA-436-4	-82.430	48.300	1986	K. Wang	CA	416.100	125	2.5
CA-8707	-79.090	48.281	1987	J-C Mareschal	CA	590.000	59	4.4
CA-8706	-79.097	48.280	1987	J-C Mareschal	CA	590.000	59	3.6
CA-9105	-78.437	48.251	1991	J-C Mareschal	CA	429.963	46	3.6
CA-0011	-89.483	48.196	2000	J-C Mareschal	CA	470.000	44	2.8
CA-0010	-89.484	48.194	2000	J-C Mareschal	CA	480.000	48	2.8
CA-9103	-77.599	48.139	1991	J-C Mareschal	CA	360.041	46	3.6
CA-9101	-77.582	48.129	1991	J-C Mareschal	CA	316.496	33	3.7
CA-9001	-77.749	48.115	1990	J-C Mareschal	CA	416.791	72	3
CA-1018	-77.524	48.101	2010	J-C Mareschal	CA	1753.680	202	–
CA-8708	-77.559	48.099	1987	J-C Mareschal	CA	357.083	38	4.1
CA-8709	-77.556	48.097	1987	J-C Mareschal	CA	335.334	36	4.8
CA-113-2	-56.000	48.000	1978	A.M. Jessop	CA	518.500	33	3.06
CA-437-3	-82.410	47.940	1986	K. Wang	CA	457.800	126	4.07
US-MN5-35	-91.720	47.820	1967	R.F. Roy	US	594.600	36	1.95
US-MN5-34	-91.720	47.820	1967	R.F. Roy	US	365.900	23	1.85
DM 034	-91.703	47.809	2010	Heine & Severson	US	609.987	145	1.8

Continued on next page

Table B. 1: Supplementary metadata of 510 BTPs suitable for climate reconstructions sorted by latitude (North-South).

Name	Longitude	Latitude	Logging Year	Contact	Country	Max. Depth	Data number	Conductivity
DM 003	-91.703	47.809	2009	Heine & Severson	US	609.939	146	1.8
MEX 153	-91.731	47.809	2010	Heine & Severson	US	500.000	85	–
DM 111	-91.723	47.802	2009	Heine & Severson	US	609.926	148	1.8
DM 109	-91.735	47.800	2009	Heine & Severson	US	609.914	146	1.8
DM 116	-91.740	47.793	2009	Heine & Severson	US	606.018	145	1.8
CA-415-0	-65.880	47.720	1986	A.M. Jessop	CA	403.800	50	3.3
CA-9013	-70.095	47.695	1990	J-C Mareschal	CA	490.000	64	5.2
USA 22-24-27	-103.875	47.628	1983	Morgan	US	2845.000	314	–
CA-164-0	-69.460	47.610	1986	K. Wang	CA	600.700	38	3.99
CA-405-0	-66.300	47.560	1986	A.M. Jessop	CA	350.500	22	2.8
NDGS 5086	-103.800	47.474	1975	Scattolini	US	1950.810	128	4.01
CA-8812	-78.712	47.402	1988	J-C Mareschal	CA	357.308	45	3.5
CA-8811	-78.710	47.402	1988	J-C Mareschal	CA	387.104	45	3.7
CA-8813	-78.713	47.402	1988	J-C Mareschal	CA	389.168	45	3.1
CA-8810	-78.695	47.401	1988	J-C Mareschal	CA	420.137	43	3.3
NDSWC 3558	-101.275	47.112	1975	Scattolini	US	301.750	34	4.89
NDGS 2894	-103.668	47.109	1976	Scattolini	US	1981.200	152	1.3
CA-1103	-80.876	46.806	2011	J-C Mareschal	CA	943.530	100	3.255
CA-1303	-81.168	46.748	2013	J-C Mareschal	CA	610.000	61	2.245
CA-1302	-81.163	46.747	2013	J-C Mareschal	CA	790.000	78	2.289
CA-1202	-81.329	46.689	2012	J-C Mareschal	CA	942.110	81	2.649
CA-1102	-80.826	46.680	2011	J-C Mareschal	CA	929.950	93	2.724
CA-1101	-80.827	46.676	2011	J-C Mareschal	CA	1297.766	130	2.588
CA-1301	-80.809	46.671	2013	J-C Mareschal	CA	2060.000	206	2.674
CA-0316	-80.870	46.660	2003	J-C Mareschal	CA	599.800	57	2.69
CA-067-1	-81.300	46.650	1978	A.M. Jessop	CA	593.400	47	3.14
CA-067-9	-81.340	46.650	1978	A.M. Jessop	CA	356.000	12	2.85
CA-0402	-81.350	46.639	2004	J-C Mareschal	CA	2279.460	228	3
CA-067-2	-81.390	46.630	1978	A.M. Jessop	CA	593.400	37	3.13
RIO TINTO 39	-93.043	46.622	2009	Heine & Severson	US	460.985	133	2.3
CA-067-3	-81.430	46.610	1979	A.M. Jessop	CA	575.800	21	3.85
RIO TINTO 38	-93.060	46.609	2009	Heine & Severson	US	600.733	149	2.4
CA-1204	-80.882	46.564	2012	J-C Mareschal	CA	1094.421	94	2.647
CA-1201	-80.879	46.564	2012	J-C Mareschal	CA	1238.356	124	2.739

Continued on next page

Table B. 1: Supplementary metadata of 510 BTPs suitable for climate reconstructions sorted by latitude (North-South).

Name	Longitude	Latitude	Logging Year	Contact	Country	Max. Depth	Data number	Conductivity
US-WA3-177	-122.800	46.530	1967	J.H. Sass	US	410.000	37	1.07
CA-067-6	-81.080	46.520	1975	K. Wang	CA	597.400	39	2.5
CA-1205	-81.552	46.509	2012	J-C Mareschal	CA	641.978	90	2.798
CA-0612	-89.250	46.500	2006	J-C Mareschal	CA	713.416	86	2.222
NDSWC 4509 (2)	-101.965	46.500	1976	Scattolini	US	320.040	22	7.23
CA-1206	-81.545	46.498	2012	J-C Mareschal	CA	804.505	90	2.809
CA-1105	-81.518	46.473	2011	J-C Mareschal	CA	898.923	90	–
CA-1304	-81.067	46.438	2013	J-C Mareschal	CA	1012.800	104	3.256
CA-8927	-81.050	46.433	1989	J-C Mareschal	CA	472.806	60	4
CA-0401	-81.309	46.433	2004	J-C Mareschal	CA	2206.770	224	3.32
CA-8926	-81.050	46.433	1989	J-C Mareschal	CA	600.000	60	4
CA-067-7	-81.320	46.430	1973	A.M. Jessop	CA	597.400	39	2.72
CA-067-5	-81.390	46.410	1975	A.M. Jessop	CA	575.500	21	2.72
CA-067-4	-81.440	46.380	1975	A.M. Jessop	CA	332.200	12	2.72
CA-056-0	-63.450	46.270	1972	A.M. Jessop	CA	401.400	25	2.36
CA-005-0	-74.020	45.820	1958	K. Wang	CA	600.200	72	2.63
CA-005-1	-74.010	45.820	1978	K. Wang	CA	594.100	76	2.63
CA-065-0	-63.450	45.780	1979	A.M. Jessop	CA	306.300	19	2.4
US-kiw82	-69.200	45.430	1982	E.R. Decker	US	600.000	59	2.9
CA-001-0	-75.720	45.400	1978	A.M. Jessop	CA	587.000	76	2.37
US-MT2-8	-109.900	45.050	1965	D.D. Blackwell	US	300.000	25	3.01
CA-051-0	-76.060	45.010	1978	A.M. Jessop	CA	318.200	10	2.5
CA-054-0	-63.480	44.920	1978	K. Wang	CA	591.000	38	4.46
CA-8911	-77.724	44.871	1989	J-C Mareschal	CA	424.778	43	2.6
CA-8910	-77.722	44.871	1989	J-C Mareschal	CA	340.271	38	2.8
CA-8907	-78.503	44.858	1989	J-C Mareschal	CA	300.000	26	4
US-luc82	-68.600	44.720	1982	E.R. Decker	US	420.000	39	2.5
CA-002-0	-63.590	44.640	1978	K. Wang	CA	333.500	23	2.1
CA-8820	-77.788	44.533	1988	J-C Mareschal	CA	377.150	41	2.8
CA-8814	-77.452	44.504	1988	J-C Mareschal	CA	330.447	33	3.8
US-ME7-34	-68.620	44.400	1965	Birch & Roy	US	350.000	34	3.91
US-sar64	-74.270	44.330	1964	H.N. Pollack	US	368.200	36	1.84
US-sar92	-74.270	44.330	1992	E.R. Decker	US	368.200	91	1.84
US-NY6-14	-75.400	44.270	1969	Urban	US	335.300	42	4.98

Continued on next page

Table B. 1: Supplementary metadata of 510 BTPs suitable for climate reconstructions sorted by latitude (North-South).

Name	Longitude	Latitude	Logging Year	Contact	Country	Max. Depth	Data number	Conductivity
US-NY6-13	-75.400	44.270	1969	Urban	US	312.400	35	4.98
US-NY6-11	-75.420	44.250	1969	Urban	US	334.600	41	4.02
US-wad64	-73.470	44.230	1965	H.N. Pollack	US	368.200	35	1.84
US-ME7-35	-70.620	44.050	1964	Birch & Roy	US	300.000	23	3.4
US-WY2-27	-109.200	43.870	1966	D.D. Blackwell	US	450.000	39	2.92
CA-8901	-78.717	43.868	1989	J-C Mareschal	CA	300.000	29	2.5
CA-018-1	-66.000	43.760	1986	K. Wang	CA	480.000	93	3.03
CA-018-0	-66.000	43.760	1986	A.M. Jessop	CA	470.000	89	3.03
US-wes64	-72.820	43.280	1964	H.N. Pollack	US	410.100	27	2.65
US-IA7-33	-95.190	43.170	1967	R.F. Roy	US	600.000	27	2.21
US-NH7-72	-72.130	42.780	1965	F. Birch	US	300.000	29	3.22
US-WY3-184	-109.500	42.770	1966	J.H. Sass	US	594.360	34	3.02
US-NY6-43	-76.900	42.420	1969	Urban	US	395.800	49	2.01
TRAVIS #1	-103.502	41.358	1982	Jim and Larry	US	510.000	48	–
US-NJ6-8	-74.580	41.100	1969	W.H. Diment	US	594.400	75	2.9
US-NJ6-10	-74.600	41.080	1960	W.H. Diment	US	579.100	19	2.89
B13-9P	-101.510	40.151	1982	Morgan	US	1320.000	264	–
26057211310000	-101.510	40.150	1982	Larry/Jim	US	515.000	50	–
US-UT3-172	-109.600	39.980	1969	J.H. Sass	US	594.360	42	2.36
US-CO3-75	-108.400	39.970	1969	J.H. Sass	US	304.800	33	1.43
US-CO5-25	-108.300	39.950	1966	R.F. Roy	US	310.000	12	0.87
US-CO5-6	-105.500	39.870	1967	Decker & Birch	US	375.000	18	2.47
US-CO5-20	-105.200	39.780	1964	Roy & Decker	US	530.000	52	3.01
US-CA3-25	-122.800	39.700	1969	J.H. Sass	US	327.050	37	4.31
US-CO5-22	-106.100	39.430	1967	Decker & Birch	US	510.000	36	3.5
US-NV3-141	-118.300	39.200	1966	J.H. Sass	US	317.400	61	2.87
US-NV3-138	-118.300	39.200	1966	J.H. Sass	US	325.000	59	2.95
US-NV7-68	-114.900	39.070	1965	R.F. Roy	US	360.000	29	3.29
US-DC6-62	-77.000	39.000	1963	W.H. Diment	US	593.320	21	3.11
US-DC6-61	-77.000	39.000	1963	W.H. Diment	US	598.930	22	2.93
US-DC6-63	-77.000	39.000	1963	W.H. Diment	US	597.740	19	2.92
US-CA7-28	-120.600	38.870	1965	R.F. Roy	US	350.000	33	3.7
US-CA7-29	-121.100	38.830	1965	R.F. Roy	US	350.000	32	2.91
US-UTSRS-3	-109.320	38.800	1979	R.N. Harris	US	495.000	93	4.82

Continued on next page

Table B. 1: Supplementary metadata of 510 BTPs suitable for climate reconstructions sorted by latitude (North-South).

Name	Longitude	Latitude	Logging Year	Contact	Country	Max. Depth	Data number	Conductivity
US-UTSRD-4	-109.870	38.730	1979	R.N. Harris	US	310.000	53	3.86
US-UTSRD-3	-109.850	38.710	1979	R.N. Harris	US	330.000	55	3.86
US-UTSRD-7	-109.480	38.690	1980	R.N. Harris	US	370.000	71	3.86
US-CO5-8	-106.500	38.680	1967	Decker & Birch	US	480.000	42	2.8
US-UTSRD-1	-109.670	38.610	1979	R.N. Harris	US	390.000	63	3.86
US-UTSRD-2	-109.620	38.580	1976	R.N. Harris	US	355.000	28	3.86
US-NV7-55	-117.300	38.320	1965	R.F. Roy	US	330.000	31	3.17
ROSCOE	-93.743	37.999	1984	Gosnold	US	490.000	45	–
US-NV3-120	-114.500	37.970	1970	J.H. Sass	US	388.620	26	3.88
US-CO5-23	-107.600	37.930	1967	Decker & Birch	US	375.000	28	3.87
US-NV3-91	-116.200	37.180	1963	J.H. Sass	US	320.040	19	4.9
US-CA3-41	-118.900	37.130	1966	A.H. Lachenbruch	US	502.630	49	2.97
US-CA3-43	-119.300	37.100	1967	A.H. Lachenbruch	US	491.490	94	2.53
US-VA6-60	-77.900	36.870	1964	W.H. Diment	US	312.420	39	3.27
US-NM5-52	-105.400	36.720	1967	F. Birch	US	580.000	26	2.85
US-NM3-160	-107.200	36.680	1967	F. Birch	US	579.120	19	2.76
US-NV7-47	-115.100	35.480	1965	R.F. Roy	US	315.000	14	3.49
US-NV7-48	-115.100	35.380	1965	R.F. Roy	US	300.000	14	3.64
US-CA3-38	-119.300	35.270	1969	J.H. Sass	US	600.000	20	1.77
US-AZ7-17	-114.300	33.630	1967	R.F. Roy	US	410.000	39	3.32
US-ALclay6	-86.800	33.500	1993	S.R. Durrans	US	300.000	83	2.03
US-SC6-53	-81.670	33.280	1963	W.H. Diment	US	327.660	24	2.57
US-SC6-52	-81.670	33.280	1963	W.H. Diment	US	594.360	55	2.57
US-AZ3-6	-110.600	33.030	1963	J.H. Sass	US	320.040	18	3.19
US-AZ3-8	-111.000	31.970	1965	J.H. Sass	US	335.280	19	3.39
US-AZ7-25	-111.100	31.880	1965	R.F. Roy	US	400.000	20	2.68
US-AZ7-24	-111.100	31.880	1965	R.F. Roy	US	400.000	20	2.7
US-AZ7-23	-111.100	31.880	1965	R.F. Roy	US	450.000	22	2.87
US-AZ7-12	-110.800	31.870	1965	R.F. Roy	US	320.000	27	3.1
US-AZ7-20	-110.700	31.830	1965	R.F. Roy	US	460.000	22	3.46
CU-BJ-55	-82.030	23.190	1981	Vladimir Cermak	CU	500.000	43	1.61
CU-VB-1	-82.090	23.180	1991	Vladimir Cermak	CU	330.000	31	1.61
CU-C-357	-76.940	20.040	1991	Vladimir Cermak	CU	491.420	44	2.6
US-PR6-66	-67.170	18.150	1963	W.H. Diment	US	304.800	37	2.51

REFERENCES

2k Consortium, P. (2013). Continental-scale temperature variability during the past two millennia. *Nature Geoscience*, *6*(5), 339–346. Progress Article.

Allan, R. P., Liu, C., Loeb, N. G., Palmer, M. D., Roberts, M., Smith, D. and Vidale, P.-L. (2014). Changes in global net radiative imbalance 1985–2012. *Geophysical Research Letters*, *41*(15), 5588–5597. http://dx.doi.org/10.1002/2014GL060962

Bartlett, M. G., Chapman, D. S. and Harris, R. N. (2004). Snow and the ground temperature record of climate change. *Journal of Geophysical Research (Earth Surface)*, *109*, F04008. http://dx.doi.org/10.1029/2004JF000224

Bauer, S. E., Bausch, A., Nazarenko, L., Tsigaridis, K., Xu, B., Edwards, R., Bisiaux, M. and McConnell, J. (2013). Historical and future black carbon deposition on the three ice caps: Ice core measurements and model simulations from 1850 to 2100. *Journal of Geophysical Research: Atmospheres*, *118*(14), 7948–7961. http://dx.doi.org/10.1002/jgrd.50612

Beck, A. E. (1977). Climatically perturbed temperature gradient and their effect on regional and continental heat-flow means. *Tectonophysics*, *41*(1-3), 17–39.

Beck, A. E., Shen, P. Y., Beltrami, H., Mareschal, J.-C., Šafanda, J., Sebagenzi, M. N., Vasseur, G. and Wang, K. (1992). A comparison of five different analyses in the interpretation of five borehole temperature data sets. *Palaeogeography, Palaeoclimatology, Palaeoecology*, *98*(2), 101–112. http://dx.doi.org/10.1016/0921-8181(92)90029-A

Beltrami, H. and Bourlon, E. (2004). Ground warming patterns in the Northern Hemisphere during the last five centuries. *Earth and Planetary Science Letters*, *227*(3), 169–177. http://dx.doi.org/doi:10.1016/j.epsl.2004.09.014

Beltrami, H., Gosselin, C. and Mareschal, J. C. (2003). Ground surface temperatures in Canada: Spatial and temporal variability. *Geophysical research letters*, *30*(10). http://dx.doi.org/10.1029/2003GL017144

Beltrami, H., Jessop, A. M. and Mareschal, J.-C. (1992). Ground temperature histories in eastern and central Canada from geothermal measurements: evidence of climatic change. *Global and planetary change*, *6*(2), 167–183. http://dx.doi.org/10.1016/0921-8181(92)90033-7

Beltrami, H. and Mareschal, J.-C. (1992). Ground temperature histories for central and eastern canada from geothermal measurements: Little ice age signature. *Geophysical Research Letters*, *19*(7), 689–692. http://dx.doi.org/10.1029/92GL00671

Beltrami, H. and Mareschal, J.-C. (1993). Ground temperature changes in eastern canada: borehole temperature evidence compared with proxy data. *Terra Nova*, *5*(1), 21–28. http://dx.doi.org/10.1111/j.1365-3121.1993.tb00222.x

Beltrami, H., Matharoo, G. S. and Smerdon, J. E. (2015). Ground surface temperature and continental heat gain: uncertainties from underground. *Environmental Research Letters*, *10*(1), 014009. Available from: http://stacks.iop.org/1748-9326/10/i=1/a=014009

Beltrami, H., Matharoo, G. S., Tarasov, L., Rath, V. and Smerdon, J. E. (2014). Numerical studies on the impact of the last glacial cycle on recent borehole temperature profiles: implications for terrestrial energy balance. *Climate of the Past*, *10*(5), 1693–1706. http://dx.doi.org/10.5194/cp-10-1693-2014

Beltrami, H., Smerdon, J. E., G.S.Matharoo and N.Nickerson (2011). Impact of maximum borehole depths on inverted temperature histories in borehole paleoclimatology. *Climate of the Past*, *7*, 715–748. http://dx.doi.org/10.5194/cp-7-745-2011

Benfield, A. E. (1939). Terrestrial heat flow in Great Britain. *Proceedings of the Royal Society London A*, *173*, 428–450.

Bodri, L. and Cermak, V. (2007). *Borehole Climatology*. Amsterdam: Elsevier.

Briffa, K. R., Bartholin, T. S., Eckstein, D., Jones, P. D., Karlén, W., Schweingruber, F. H. and Zetterberg, P. (1990). A 1,400-year tree-ring record of summer temperatures in fennoscandia. *Nature*. http://dx.doi.org/10.1038/346434a0

Briffa, K. R. and Osborn, T. J. (1999). Seeing the wood from the trees. *Science*, *284*(5416), 926–927. http://dx.doi.org/10.1126/science.284.5416.926

Bullard, E. C. (1939). Heat Flow in South Africa. *Proceedings of the Royal Society London A*, *173*, 474–502.

Carslaw, H. S. and Jaeger, J. C. (1959). *Conduction of Heat in Solids*. New York: Oxford Science Publications.

Cermak, V. (1971). Underground temperature and inferred climatic temperature of the past millenium. *Palaeogeography, Palaeoclimatology, Palaeoecology*, *10*, 1–19.

Chouinard, C., Fortier, R. and Mareschal, J.-C. (2007). Recent climate variations in the subarctic inferred from three borehole temperature profiles in northern Quebec, Canada. *Earth and Planetary Science Letters*, *263*(3), 355–369. http://dx.doi.org/10.1016/j.epsl.2007.09.017

Chouinard, C. and Mareschal, J.-C. (2007). Selection of borehole temperature depth profiles for regional climate reconstructions. *Climate of the Past*, *3*(2), 297–313. http://dx.doi.org/10.5194/cp-3-297-2007

Clauser, C. and Mareschal, J.-C. (1995). Ground temperature history in central Europe from borehole temperature data. *Geophysical Journal International*, *121*(3), 805–817. http://dx.doi.org/10.1111/j.1365-246X.1995.tb06440.x

Davis, B., Brewer, S., Stevenson, A. and Guiot, J. (2003). The temperature of europe during the holocene reconstructed from pollen data. *Quaternary Science Reviews*, *22*(15–17), 1701 – 1716. http://dx.doi.org/10.1016/S0277-3791(03)00173-2

Douglass, A. E. (1919). *Climatic cycles and tree-growth*, volume 1. Carnegie Institution of Washington.

Gajewski, K. (2015). Quantitative reconstruction of holocene temperatures across the canadian arctic and greenland. *Global and Planetary Change*, *128*, 14 – 23. http://dx.doi.org/10.1016/j.gloplacha.2015.02.003

García-García, A., Cuesta-Valero, F. J., Beltrami, H. and Smerdon, J. E. (2016). Simulation of air and ground temperatures in pmip3/cmip5 last millennium simulations: implications for climate reconstructions from borehole temperature profiles. *Environmental Research Letters*, *11*(4), 044022. Available from: http://stacks.iop.org/1748-9326/11/i=4/a=044022

George, S. S. and Ault, T. R. (2014). The imprint of climate within northern hemisphere trees. *Quaternary Science Reviews*, *89*, 1 – 4. http://dx.doi.org/10.1016/j.quascirev.2014.01.007

González-Rouco, J. F., Beltrami, H., Zorita, E. and Stevens, M. B. (2009). Borehole climatology: a discussion based on contributions from climate modeling. *Climate of the Past*, *5*(1), 97–127. http://dx.doi.org/10.5194/cp-5-97-2009

González-Rouco, J. F., Beltrami, H., Zorita, E. and von Storch, H. (2006). Simulation and inversion of borehole temperature profiles in surrogate climates: Spatial distribution and surface coupling. *Geophysical Research Letters*, *33*(1), n/a–n/a. L01703, http://dx.doi.org/10.1029/2005GL024693. Available from: http://dx.doi.org/10.1029/2005GL024693

Gosnold, W., Todhunter, P. and Schmidt, W. (1997). The borehole temperature record of climate warming in the mid-continent of north america. *Global and Planetary Change*, *15*(1–2), 33 – 45. http://dx.doi.org/http://dx.doi.org/10.1016/S0921-8181(97)00002-7

Gosselin, C. and Mareschal, J.-C. (2003a). Recent warming in northwestern ontario inferred from borehole temperature profiles. *Journal of Geophysical Research: Solid Earth*, *108*(B9), n/a–n/a. 2452, http://dx.doi.org/10.1029/2003JB002447

Gosselin, C. and Mareschal, J.-C. (2003b). Variations in ground surface temperature histories in the Thompson Belt, Manitoba, Canada: environment and climate changes. *Global and Planetary Change*, *39*(3–4), 271–284. http://dx.doi.org/http://dx.doi.org/10.1016/S0921-8181(03)00120-6

Guillou-Frottier, L., Mareschal, J.-C. and Musset, J. (1998). Ground surface temperature history in central Canada inferred from 10 selected borehole temperature profiles. *Journal of Geophysical Research: Solid Earth (1978–2012)*, *103*(B4), 7385–7397. http://dx.doi.org/10.1029/98JB00021

Gullett, D. and Skinner, W. (1992). *state of Canada's climate.* Environment Canada.

Hansen, J., Nazarenko, L., Ruedy, R., Sato, M., Willis, J., Del Genio, A., Koch, D., Lacis, A., Lo, K., Menon, S., Novakov, T., Perlwitz, J., Russell, G., Schmidt, G. A. and Tausnev, N. (2005). Earth's energy imbalance: Confirmation and implications. *Science*, *308*(5727), 1431–1435. http://dx.doi.org/10.1126/science.1110252

Hansen, J., Ruedy, R., Sato, M. and Lo, K. (2010). Global surface temperature change. *Reviews of Geophysics*, *48*(4), n/a–n/a. RG4004, http://dx.doi.org/10.1029/2010RG000345

Hansen, J., Sato, M., Kharecha, P. and von Schuckmann, K. (2011). Earth's energy imbalance and implications. *Atmospheric Chemistry and Physics*, *11*(24), 13421–13449. http://dx.doi.org/10.5194/acp-11-13421-2011

Harris, R. N. and Chapman, D. S. (1998a). Geothermics and climate change: 1. analysis of borehole temperatures with emphasis on resolving power. *Journal of Geophysical Research: Solid Earth*, *103*(B4), 7363–7370. http://dx.doi.org/10.1029/97JB03297

Harris, R. N. and Chapman, D. S. (1998b). Geothermics and climate change: 2. joint analysis of borehole temperature and meteorological data. *Journal of Geophysical Research: Solid Earth*, *103*(B4), 7371–7383. http://dx.doi.org/10.1029/97JB03296

Harris, R. N. and Chapman, D. S. (2001). Mid-latitude (30–60 n) climatic warming inferred by combining borehole temperatures with surface air temperatures. *Geophysical Research Letters*, *28*(5), 747–750. http://dx.doi.org/10.1029/2000GL012348

Hotchkiss, W. O. and Ingersoll, L. R. (1934). Post-glacial time calculations from recent geothermal measurements in the Calumet Copper Mines. *Journal of Geology, 42*, 113–142.

Huang, S., Pollack, H. and Shen, P. (1999). Global database of borehole temperatures and climate reconstructions. *PAGES Newsl, 7*(2), 18–19.

Huang, S., Pollack, H. N. and Shen, P.-Y. (2000). Temperature trends over the past five centuries reconstructed from borehole temperatures. *Nature, 403*(6771), 756–758. http://dx.doi.org/10.1038/35001556

Jackson, D. D. (1972). Interpretation of inaccurate, insufficient, and inconsistent data. *Geophysical Journal International, 28*, 97–110.

Jacques, J.-M. S., Cumming, B. F., Sauchyn, D. J. and Smol, J. P. (2015). The bias and signal attenuation present in conventional pollen-based climate reconstructions as assessed by early climate data from minnesota, usa. *PloS one, 10*(1), e0113806. http://dx.doi.org/10.1371/journal.pone.0113806

Jaume-Santero, F., Beltrami, H. and Mareschal, J.-C. (2016). North American borehole temperature profiles suitable for climate studies. http://dx.doi.org/10.6084/m9.figshare.2062140. Available from: https://dx.doi.org/10.6084/m9.figshare.2062140.v1

Jaupart, C. and Mareschal, J.-C. (2011). *Heat generation and transport in the Earth.* Cambridge University Press.

Jaupart, C. and Mareschal, J. C. (2015). Heat flow and the structure of the lithosphere. In A. B. Watts (dir.), *Treatise on Geophysics, vol. 6, 2nd edition* chapitre 5, 217–253. New York: Elsevier.

Jones, P. D., Lister, D. H., Osborn, T. J., Harpham, C., Salmon, M. and Morice, C. P. (2012). Hemispheric and large-scale land-surface air temperature variations: An extensive revision and an update to 2010. *Journal of Geophysical Research: Atmospheres*, *117*(D5), n/a–n/a. D05127, http://dx.doi.org/10.1029/2011JD017139

Kueppers, L. M., Snyder, M. A. and Sloan, L. C. (2007). Irrigation cooling effect: Regional climate forcing by land-use change. *Geophysical Research Letters*, *34*(3), n/a–n/a. L03703, http://dx.doi.org/10.1029/2006GL028679

Kukkonen, I. T. and Jõeleht, A. (2003). Weichselian temperatures from geothermal heat flow data. *Journal of Geophysical Research: Solid Earth*, *108*(B3). http://dx.doi.org/10.1029/2001JB001579

Lachenbruch, A. H. and Marshall, B. V. (1986). Changing climate: Geothermal evidence from permafrost in the Alaskan Arctic. *Science*, *234*, 689–696.

Lanczos, C. (1961). *Linear Differential Operators*. Princeton, N.J.: D. Van Nostrand.

Lane, A. C. (1923). Geotherms of lake superior copper country. *Geological Society of America Bulletin*, *34*(4), 703–720. http://dx.doi.org/10.1130/GSAB-34-703. Available from: http://gsabulletin.gsapubs.org/content/34/4/703.abstract

Lewis, T. (1992). Climate change inferred from underground temperatures. *Paleogeogr. Paleoclimatol. Paleoecol.*, *98*, 71–281.

Lewis, T. J. and Wang, K. (1998). Geothermal evidence for deforestation induced warming: Implications for the Climatic impact of land development. *Geophysical Research Letters*, *25*(4), 535–538. http://dx.doi.org/10.1029/98GL00181

Majorowicz, J., Safanda, J. and Skinner, W. (2002). East to west retardation in the onset of the recent warming across canada inferred from inversions of temperature logs. *Journal of Geophysical Research: Solid Earth, 107*(B10), ETG 6–1–ETG 6–12. 2227, http://dx.doi.org/10.1029/2001JB000519

Majorowicz, J. A. and Safanda, J. (2001). Composite surface temperature history from simultaneous inversion of borehole temperatures in western canadian plains. *Global and Planetary Change, 29*(3–4), 231 – 239. Inference of Climate Change from Geothermal Data, http://dx.doi.org/10.1016/S0921-8181(01)00092-3

Mann, M. E., Zhang, Z., Hughes, M. K., Bradley, R. S., Miller, S. K., Rutherford, S. and Ni, F. (2008). Proxy-based reconstructions of hemispheric and global surface temperature variations over the past two millennia. *Proceedings of the National Academy of Sciences, 105*(36), 13252–13257.

Mann, M. E., Zhang, Z., Rutherford, S., Bradley, R. S., Hughes, M. K., Shindell, D., Ammann, C., Faluvegi, G. and Ni, F. (2009). Global signatures and dynamical origins of the little ice age and medieval climate anomaly. *Science, 326*(5957), 1256–1260. http://dx.doi.org/10.1126/science.1177303

Mareschal, J.-C. and Beltrami, H. (1992). Evidence for recent warming from perturbed geothermal gradients: examples from eastern Canada. *Climate Dynamics, 6*(3-4), 135–143. http://dx.doi.org/10.1007/BF00193525

Mareschal, J.-C., Rolandone, F. and Bienfait, G. (1999). Heat flow variations in a deep borehole near Sept-Iles, Québec, Canada: Paleoclimatic interpretation and implications for regional heat flow estimates. *Geophysical Research Letters, 26*(14), 2049–2052. http://dx.doi.org/10.1029/1999GL900489

Masson-Delmotte, V., Schulz, M., Abe-Ouchi, A., Beer, J., Ganopolski, A.,

González Rouco, J., Jansen, E., Lambeck, K., Luterbacher, J., Naish, T. *et al.* (2013). 2013: Information from paleoclimate archives. in: Climate change 2013: The physical science basis. contribution of working group i to the fifth assessment report of the intergovernmental panel on climate change. *IPCC, Fifth Assessment Report*, 383–464.

McKay, N. (2014). A novel multiproxy approach: The pages north america 2k working group. *PAGES magazine*, *22*(2), 100.

Moberg, A., Sonechkin, D. M., Holmgren, K., Datsenko, N. M. and Karlén, W. (2005). Highly variable northern hemisphere temperatures reconstructed from low-and high-resolution proxy data. *Nature*, *433*(7026), 613–617. `http://dx.doi.org/10.1038/nature03265`

Morice, C. P., Kennedy, J. J., Rayner, N. A. and Jones, P. D. (2012). Quantifying uncertainties in global and regional temperature change using an ensemble of observational estimates: The hadcrut4 data set. *Journal of Geophysical Research: Atmospheres*, *117*(D8), n/a–n/a. D08101, `http://dx.doi.org/10.1029/2011JD017187`. Available from: `http://dx.doi.org/10.1029/2011JD017187`

Mosegaard, K. and Tarantola, A. (1995). Monte carlo sampling of solutions to inverse problems. *Journal of Geophysical Research: Solid Earth*, *100*(B7), 12431–12447. `http://dx.doi.org/10.1029/94JB03097`

Oeschger, H. and Langway, C. J. (1989). *The environmental record in glaciers and ice sheets*. New York, NY (US); Wiley-Interscience.

PAGES 2k-PMIP3 group (2015). Continental-scale temperature variability in pmip3 simulations and pages 2k regional temperature reconstructions over the

past millennium. *Climate of the Past*, *11*, 1673–1699. http://dx.doi.org/10.5194/cp-11-1673-2015

Parker, R. L. (1977). Understanding inverse theory. *Annual Review of Earth and Planetary Sciences*, *5*, 35.

Parker, R. L. (1994). *Geophysical inverse theory*. Princeton university press.

Pickler, C.,-Beltrami, H. and Mareschal, J.-C. (2016a). Climate trends in northern ontario and quebec from borehole temperature profiles. *Climate of the Past Discussions*, *2016*, 1–21. http://dx.doi.org/10.5194/cp-2016-55. Available from: http://www.clim-past-discuss.net/cp-2016-55/

Pickler, C., Beltrami, H. and Mareschal, J.-C. (2016b). Laurentide ice sheet basal temperatures during the last glacial cycle as inferred from borehole data. *Climate of the Past*, *12*(1), 115–127. http://dx.doi.org/10.5194/cp-12-115-2016

Pollack, H. N. and Smerdon, J. E. (2004). Borehole climate reconstructions: Spatial structure and hemispheric averages. *Journal of Geophysical Research: Atmospheres*, *109*(D11), n/a–n/a. D11106, http://dx.doi.org/10.1029/2003JD004163. Available from: http://dx.doi.org/10.1029/2003JD004163

Putnam, S. N. and Chapman, D. S. (1996). A geothermal climate change observatory: First year results from Emigrant Pass in northwest Utah. *Journal of Geophysical Research (Solid Earth)*, *101*, 21. http://dx.doi.org/10.1029/96JB01903

Sass, J. H., Lachenbruch, A. H. and Jessop, A. M. (1971). Uniform heat flow in a deep hole in the Canadian Shield and its paleoclimatic implications. *Journal of Geophysical Research*, *76*(35), 8586–8596. http://dx.doi.org/10.1029/JB076i035p08586

Scattolini, R. (1978). *Heat flow and heat production studies in North Dakota.* (Thèse de doctorat). University of North Dakota.

Schmidt, G. A., Kelley, M., Nazarenko, L., Ruedy, R., Russell, G. L., Aleinov, I., Bauer, M., Bauer, S. E., Bhat, M. K., Bleck, R., Canuto, V., Chen, Y.-H., Cheng, Y., Clune, T. L., Del Genio, A., de Fainchtein, R., Faluvegi, G., Hansen, J. E., Healy, R. J., Kiang, N. Y., Koch, D., Lacis, A. A., LeGrande, A. N., Lerner, J., Lo, K. K., Matthews, E. E., Menon, S., Miller, R. L., Oinas, V., Oloso, A. O., Perlwitz, J. P., Puma, M. J., Putman, W. M., Rind, D., Romanou, A., Sato, M., Shindell, D. T., Sun, S., Syed, R. A., Tausnev, N., Tsigaridis, K., Unger, N., Voulgarakis, A., Yao, M.-S. and Zhang, J. (2014). Configuration and assessment of the giss modele2 contributions to the cmip5 archive. *Journal of Advances in Modeling Earth Systems*, *6*(1), 141–184. http://dx.doi.org/10.1002/2013MS000265. Available from: http://dx.doi.org/10.1002/2013MS000265

Shen, P. Y. and Beck, A. E. (1991). Least squares inversion of borehole temperature measurements in functional space. *Journal of Geophysical Research: Solid Earth*, *96*(B12), 19965–19979. http://dx.doi.org/10.1029/91JB01883

Skinner, W. R. and Majorowicz, J. A. (1999). Regional climatic warming and associated twentieth century land-cover changes in north-western north america. *Climate Research*, *12*(1), 39–52. http://dx.doi.org/10.3354/cr012039

Smith, D. M., Allan, R. P., Coward, A. C., Eade, R., Hyder, P., Liu, C., Loeb, N. G., Palmer, M. D., Roberts, C. D. and Scaife, A. A. (2015). Earth's energy imbalance since 1960 in observations and cmip5 models. *Geophysical Research Letters*, *42*(4), 1205–1213. 2014GL062669, http://dx.doi.org/10.1002/2014GL062669

Stevens, M. B., González-Rouco, J. F. and Beltrami, H. (2008). North american

climate of the last millennium: Underground temperatures and model comparison. *Journal of Geophysical Research: Earth Surface*, *113*(F1), n/a–n/a. F01008, http://dx.doi.org/10.1029/2006JF000705

Tarantola, A. and Valette, B. (1982). Generalized nonlinear inverse problems solved using the least squares criterion. *Rev. Geophys. Space Phys*, *20*(2), 219–232.

Thompson, L. G., Mosley-Thompson, E., Davis, M. E., Zagorodnov, V. S., Howat, I. M., Mikhalenko, V. N. and Lin, P.-N. (2013). Annually resolved ice core records of tropical climate variability over the past 1800 years. *Science*, *340*(6135), 945–950. http://dx.doi.org/10.1126/science.1234210

Tikhonov, A. N. and Arsenin, V. Y. (1977). *Solutions of ill-posed problems*. New-York: Wiley.

Trenberth, K. E., Fasullo, J. T. and Balmaseda, M. A. (2014). Earth's energy imbalance. *Journal of Climate*, *27*(9), 3129–3144. http://dx.doi.org/dx.doi.org/10.1175/JCLI-D-13-00294.1

Trouet, V., Diaz, H. F., Wahl, E. R., Viau, A. E., Graham, R., Graham, N. and Cook, E. R. (2013). A 1500-year reconstruction of annual mean temperature for temperate north america on decadal-to-multidecadal time scales. *Environmental Research Letters*, *8*(2), 024008. Available from: http://stacks.iop.org/1748-9326/8/i=2/a=024008

Vasseur, G., Bernard, P., de Meulebrouck, J. V., Kast, Y. and Jolivet, J. (1983). Holocene paleotemperatures deduced from geothermal measurements. *Palaeogeography, Palaeoclimatology, Palaeoecology*, *43*(3–4), 237–259. http://dx.doi.org/10.1016/0031-0182(83)90013-5

Viau, A. and Gajewski, K. (2009). Reconstructing millennial-scale, regional paleoclimates of boreal canada during the holocene. *Journal of Climate*, *22*(2), 316–330. http://dx.doi.org/http://dx.doi.org/10.1175/2008JCLI2342.1

Viau, A., Ladd, M. and Gajewski, K. (2012). The climate of north america during the past 2000 years reconstructed from pollen data. *Global and Planetary Change*, *84–85*, 75 – 83. Perspectives on Climate in Medieval Time, http://dx.doi.org/10.1016/j.gloplacha.2011.09.010

Viau, A. E., Gajewski, K., Sawada, M. C. and Fines, P. (2006). Millennial-scale temperature variations in north america during the holocene. *Journal of Geophysical Research: Atmospheres*, *111*(D9), n/a–n/a. D09102, http://dx.doi.org/10.1029/2005JD006031

von Schuckmann, K., Palmer, M., Trenberth, K., Cazenave, A., Chambers, D., Champollion, N., Hansen, J., Josey, S., Loeb, N., Mathieu, P.-P. *et al.* (2016). An imperative to monitor earth's energy imbalance. *Nature Climate Change*, *6*(2), 138–144. http://dx.doi.org/doi:10.1038/nclimate2876